applied sciences

MDPI

Review

Beyond the Calcium Score: What Additional Information from a CT Scan Can Assist in Cardiovascular Risk Assessment?

Federico Bernardini [1], Martina Gelfusa [1], Mihail Celeski [1], Federica Coletti [1], Annunziata Nusca [1,*], Domenico De Stefano [2], Francesco Piccirillo [1], Fabio Mangiacapra [1], Paolo Gallo [1], Valeria Cammalleri [1], Nino Cocco [1], Raffaele Rinaldi [1], Carlo Cosimo Quattrocchi [2], Gian Paolo Ussia [1] and Francesco Grigioni [1]

[1] Unit of Cardiac Sciences, Department of Medicine, Campus Bio-Medico University of Rome, 00128 Rome, Italy
[2] Unit of Diagnostic Imaging, Department of Medicine, Campus Bio-Medico University of Rome, 00128 Rome, Italy
* Correspondence: a.nusca@policlinicocampus.it

Abstract: Coronary artery disease (CAD) still represents a leading cause of mortality worldwide. Early identification of patients at the highest risk of CAD is crucial to prevent acute adverse events and reduce morbidity and mortality. The coronary artery calcium (CAC) score is a reliable cardiovascular (CV) risk index with an independent prognostic value. Guidelines recommend using it as a risk enhancer in individuals with low or moderate CV risk. However, other computed tomography (CT) measurable parameters have recently been proposed as CV risk markers. Increasing evidence demonstrates the association between epicardial fat volume and coronary atherosclerosis in chronic and acute coronary syndromes. Furthermore, other parameters obtainable from CT, such as aortic stiffness, liver fat, aortic calcium, and myocardial scarring, are under investigation. This review aims to describe all CT potential in atherosclerosis detection and cardiovascular risk assessment beyond the CAC, trying to understand how to integrate CT parameters with traditional risk factors and to improve clinicians' ability to detect CAD early, allowing appropriate therapies promptly.

Keywords: cardiac computed tomography (CCT); cardiovascular (CV) risk; coronary artery calcium (CAC) score; epicardial adipose tissue (EAT); coronary atherosclerosis

Citation: Bernardini, F.; Gelfusa, M.; Celeski, M.; Coletti, F.; Nusca, A.; De Stefano, D.; Piccirillo, F.; Mangiacapra, F.; Gallo, P.; Cammalleri, V.; et al. Beyond the Calcium Score: What Additional Information from a CT Scan Can Assist in Cardiovascular Risk Assessment? *Appl. Sci.* **2023**, *13*, 241. https://doi.org/10.3390/app13010241

Academic Editor: Julio Garcia Flores

Received: 30 November 2022
Revised: 20 December 2022
Accepted: 23 December 2022
Published: 25 December 2022

Coronary artery disease (CAD) still represents the first cause of death worldwide, and its prevention (primary and secondary) has become a current health priority [1].

Estimating total cardiovascular (CV) risk is essential because it allows recognizing patients who could benefit most from prevention models [2]. In apparently healthy individuals, CV risk is composed of multiple risk factors (smoking habits, hypertension, diabetes mellitus, obesity, dyslipidemia, and family history of cardiovascular diseases) that interplay synergistically [3]. Therefore, various score systems including these CV risk factors have been developed for global risk estimation; the most used is the systematic coronary risk evaluation (SCORE) model and two variants for patients aged 40 to 69 (SCORE2) and for individuals over 70 (SCORE-OP) [4]. However, these scores have several limitations and do not allow for establishing the patient's absolute risk of developing coronary atherosclerosis.

Cardiovascular risk estimation has been improved in the last decade using imaging techniques, mainly looking for subclinical atherosclerotic disease [3]. Cardiac computed tomography angiography (CCTA) provides information on the presence and extension of coronary stenoses and plaque burden and morphology. Moreover, the coronary artery calcium (CAC) score has emerged as a marker of subclinical coronary disease in apparently healthy individuals. However, according to existing models, its predictive value is lower in patients with high or very low total CV risk [5]. Finally, epicardial fat volume, aortic stiffness, liver fat, aortic calcium, and myocardial scarring might be potential markers for the early detection of atherosclerosis and consequent CAD.

In this background, this review aims to describe all cardiac CT potential in atherosclerosis detection and CV risk assessment, focusing on the more traditional tools and emerging parameters under investigation. We also sought to provide information on integrating CT parameters with traditional risk factors to improve clinicians' ability to detect CAD promptly.

Five reviewers shortlisted studies and abstracts about CT-scan and cardiovascular risk assessment, excluding those that were not pertinent to the topic. Studies designed as randomized controlled trials, non-randomized trials, descriptive, and qualitative were included. The electronic search was performed on MEDLINE (pub-med) and conducted in English. The software used for the bibliography management was MENDELEY. Keywords and abbreviations were used for the concept of reduction/avoiding.

1. Current Role of CCTA in Clinical Practice and Guidelines

1.1. Chronic Coronary Syndromes

CCTA constitutes a first-line non-invasive tool in the diagnostic process of patients with stable chronic coronary syndromes (CCS). Nevertheless, its role in this category of patients went through a significant evolution. Indeed, the 2012 American Heart Association/American College of Cardiology (AHA/ACC) guidelines for the diagnosis and management of patients with stable ischemic heart disease (SIHD) reported that CCTA should be used as a first-line test for risk assessment only in patients with SIHD who were unable to exercise to an adequate workload (class IIa) [6]. The 2016 United Kingdom (UK) guidelines of National Institute for Health and Care Excellence (NICE) [7] recommend CCTA as the first-line diagnostic test in patients with atypical and typical angina (or electrocardiogram abnormalities suggestive of CAD in the absence of symptoms). More recently, the 2019 European Society of Cardiology (ESC) guidelines recommend CCTA (class IB) in suitable patients with low-to-intermediate clinical probability of CCS (Table 1) [8]. Indeed, the PROMISE trial demonstrated that CCTA is superior to functional testing in predicting cardiovascular events in patients with chest pain suspicious for coronary artery disease and reduces the rate of coronary angiography showing non-significant coronary artery disease [9]. Moreover, the SCOT-HEART trial in the same group of patients confirmed that using CCTA in addition to standard care resulted in a lower risk of death for CAD and reduced incidence of non-fatal myocardial infarction [10].

1.2. Acute Chest Pain

In the emergency department setting, CCTA may help rule out acute coronary syndrome (ACS) in patients with low-to-intermediate pre-test probability (PTP) due to its high negative predictive value. The 2014 American Heart Association/American College of Cardiology (AHA/ACC) guideline for the management of patients with non-ST-elevation acute coronary syndrome does not provide specific recommendations about CCTA [11]. However, CCTA is described as a more rapid and cost-effective diagnostic exam than stress myocardial perfusion imaging in low-risk patients with chest pain. In front of low-to-moderate risk of CAD and unconvincing results with cardiac troponin and/or electrocardiogram (ECG), the most recent European Society of Cardiology (ESC) guidelines for the management of acute coronary syndromes in patients presenting without persistent ST-segment elevation propose CCTA (Class IA) as a substitute to coronarography for ruling out ACS [12]. Furthermore, these recommendations advise performing CCTA (Class IB) for patients with persistent suspicion of ACS who have no return of chest pain, normal troponin values, and without electrocardiographic alterations before choosing an invasive strategy (Table 1) [12].

1.3. Plaque Burden

Several studies highlighted the optimal negative predictive value of CCTA, reporting annualized event rates ranging from 0.02% to 0.3% for short [13], intermediate [14], and long-term [15] outcomes in patients with normal CCTA. Contrarywise, the CONFIRM

(Coronary CT Angiography Evaluation for Clinical Outcomes: An InteRnational Multicenter) registry indicated a strong association between the extension and distribution of atherosclerotic plaques detected by CCTA and long-term prognosis, suggesting as the CCTA plaque burden might represent a significant predictor of patient outcomes [16].

Table 1. ESC and AHA/ACC guidelines recommendations about CCTA application in chronic coronary syndromes (CCS), acute coronary syndromes (ACS), and cardiovascular prevention.

Chronic Coronary Syndromes (CCS)	
ESC 2019	**AHA/ACC 2012**
Non-invasive functional imaging for myocardial ischemic or CCTA is recommended as the initial test to diagnose CAD in symptomatic patients in whom obstructive CAD cannot be excluded by clinical assessment alone **(I-B)**	CCTA can be useful as a first-line test for risk assessment in patients with SIHD who are unable to exercise to an adequate workload regardless of interpretability of ECG **(IIa-C)**
It is recommended that selection of the initial non-invasive diagnostic test is done based on the clinical likelihood of CAD and other patient characteristics that influence test performance, local expertise, and the availability of tests. **(I-C)**	CCTA may be reasonable for risk assessment in patients with SIHD who are able to exercise to an adequate workload but have an uninterpretable ECG **(IIb-B)**
CCTA should be considered as an alternative to invasive angiography if another non-invasive test is equivocal or non-diagnostic. **(IIa-C)**	CCTA can be useful for risk assessment in patients with SIHD who have an indeterminate result from functional testing **(IIa-C)**
Acute Coronary Syndromes (ACS)	
ESC 2020 (NSTEMI)	**AHA/ACC 2021 (chest pain)**
CCTA is recommended as an alternative to ICA to exclude ACS when there is a low-to-intermediate likelihood of CAD and when cardiac troponin and/or ECG are normal or inconclusive **(I-A)**	For intermediate-risk patients with acute chest pain and no known CAD eligible for diagnostic testing after a negative or inconclusive evaluation for ACS, CCTA is useful for exclusion of atherosclerotic plaque and obstructive CAD **(I-A)**
In patients with no recurrence of chest pain, normal ECG findings, and normal levels of cardiac troponin (preferably high sensitivity), but still with a suspected ACS, a non-invasive stress test (preferably with imaging) for inducible ischaemia or CCTA is recommended before deciding on an invasive approach. **(I-B)**	For intermediate-risk patients with acute chest pain with evidence of previous mildly abnormal stress test results, CCTA is reasonable for diagnosing obstructive CAD **(IIa-C)**
CardiovascularPrevention	
ESC 2021	**AHA/ACC 2019**
Coronary artery calcium (CAC) scoring can reclassify CVD risk in addition to conventional risk factors, and may be considered in men and women with calculated risks around decision thresholds	In intermediate-risk (7.5–20% 10-year ASCVD risk) adults or selected borderline-risk (5–7.5% 10-year ASCVD risk) adults in whom a coronary artery calcium score is measured for the purpose of making a treatment decision: -CAC scoring is zero → it is reasonable to withhold statin therapy and reassess in 5 to 10 years, as long as higher-risk conditions are absent (e.g., diabetes, family history of premature CAD, cigarette smoking); -CAC score is 1 to 99 → it is reasonable to initiate statin therapy for patients >55 years of age; -CAC score is 100 or higher → it is reasonable to initiate statin therapy **(IIa-B)**

CCS: chronic coronary syndromes; **CCTA:** coronary computed tomography angiography; **CAD:** coronary artery disease; **SIHD:** stable ischemic heart disease; **ECG:** electrocardiogram; **ACS:** acute coronary syndromes; **CVD:** cardiovascular disease; **ICA:** invasive coronary angiography; **CAC:** coronary artery calcium; **ASCVD**: atherosclerotic cardiovascular disease.

Several studies demonstrated how patients might be stratified across a risk continuum beyond a simple classification based on the presence of stenoses [17,18]. Indeed, in comparison to people without detectable plaques, the recognition of non-obstructive CAD on CCTA, which is typically undetected by stress test methodologies, has been related to an

adjusted hazard ratio for major adverse cardiac events (MACEs) among 1.6 and 7.1. [19]. Multiple studies showed that the number of segments involved is one of the best predictors of outcome, surpassing scores that only consider segments with mild or moderate stenosis [14,18]. Bittencourt et al. demonstrated that patients with nonobstructive CAD involving >4 coronary segments had a similar rate of cardiovascular death or myocardial infarction (MI) as those who had obstructive disease with ≤4 diseased segments [17]. The type of vessel involved also influences the prognosis of these patients. According to Weir-McCall et al., non-obstructive left main coronary artery disease, contrary to patients with CAD not including left main, was found to be related with a superior rate of plaque advancement and increased prevalence of high-risk plaques across the coronary artery tree. This implies that non-obstructive left main illness may serve as a potential indicator of a CAD category that is aggressive and may profit from a more aggressive therapy strategy [20].

Notably, plaque burden assessment by CCTA can be semi-quantitative, by counting the number of segments involved by atherosclerosis (segment involvement score (SIS), segment stenosis score (SSS), or CT-adapted Leaman score) [21] or quantitative through plaque burden using automated or semi-automated softwares [22].

In addition, numerous longitudinal trials have evaluated the function of quantitative coronary computed tomography (QCCTA) in the development of CAD across succedent CCTA studies in terms of disease advancement. Variations in QCCTA markers served as potential predictors for the progression of atherosclerotic plaque in the PARADIGM registry [22].

1.4. Plaque Morphology

Although the risk of plaque rupture is proportional to the extent of stenosis, it has been reported that nonobstructive lesions with typical features of plaque composition represent the majority of culprit lesions in ACS. Chang et al. realized a nested case-control study within a cohort of 25,251 patients undergoing CCTA with a follow-up of 3.4 years. ACS and non-event patients without prior CAD were matched for risk factors and CCTA-rated obstructive (≥50%) CAD [23]. Thus, separate core laboratories performed a blinded assessment of coronary lesions detected by CCTA, quantifying the percent stenosis diameter (SD), the percent plaque burden (PB), the plaque volume (PV) by composition (calcified, fibrous, fibrofatty, and necrotic core), and identifying high-risk plaques (HRP) (Figures 1 and 2). Notably, HRP was reported in 52% of ACS patients. Moreover, the authors reported higher PB and fibrofatty and necrotic PV in patients with ACS than non-event patients, regardless of stenosis severity [23].

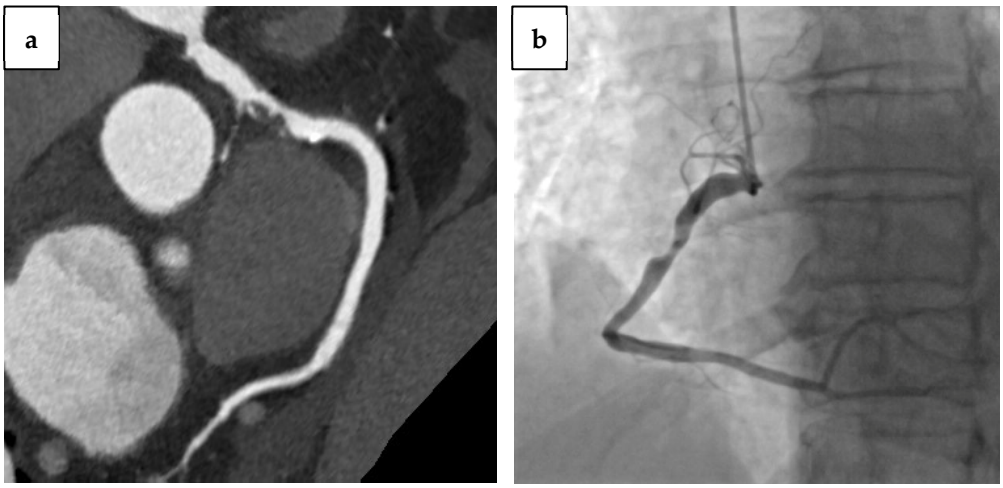

Figure 1. Right coronary artery unstable plaque: (**a**) Coronary computed tomography angiography (CCTA) assessment; (**b**) invasive coronary angiography (ICA) assessment.

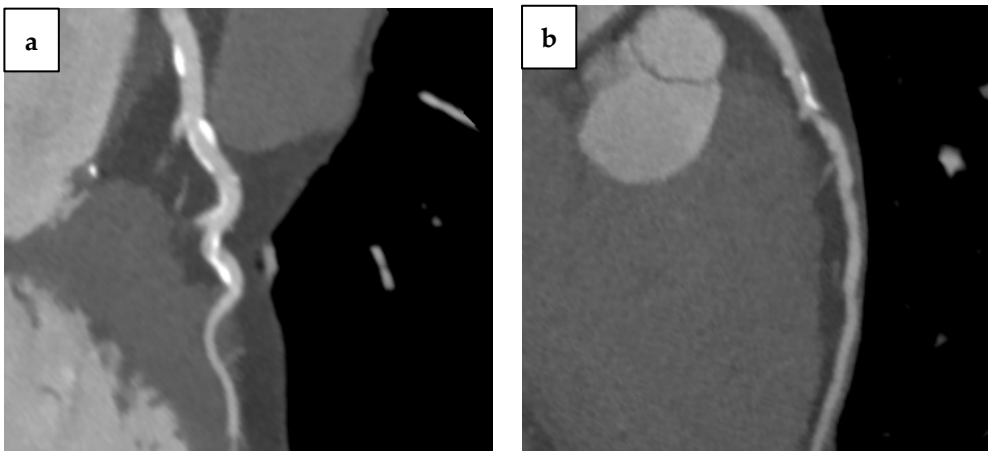

Figure 2. Coronary artery stable plaques: (**a**) calcific plaque; (**b**) fibro-calcific plaque.

From a histopathological perspective, a vulnerable plaque is defined by a thin fibrous cap, a large necrotic core, the presence of positive remodeling (PR) (remodeling index > 1.1), perivascular inflammation, and spotty calcifications. Moreover, recent studies have reported a specific attenuation pattern of atherosclerotic plaques on coronary CT images called "napkin ring sign" (NRS) [24]. It is described as a plaque core with low CT attenuation surrounded by a rim-like area of higher CT attenuation. The pathophysiology of this finding remains unclear, even if it may be linked to various high-risk characteristics such as contrast enhancement of the vasa vasorum, intraplaque hemorrhage, microcalcifications, or even healed ruptures [19]. Interestingly, Maurovich-Horvat et al., in a study involving heart donors, found that the detection of NRS at CCTA had high specificity and positive predictive value for the presence of advanced lesions [25].

Furthermore, Nakazato et al. evaluated coronary plaque characteristics with both CCTA and optical coherence tomography (OCT) [26]. They showed that PR and the presence of low-attenuation plaques (LAP) detected by CCTA are associated with thin cap fibroatheroma (TCFA) and higher macrophage infiltration evaluated by OCT. Concordantly, Hoffman et al. described a higher prevalence of remodeling in unstable plaques than in stable plaques [27]. Finally, in a sub-analysis of the NXT (HeartFlowNXT: HeartFlow Analysis of Coronary Blood Flow Using Coronary CT Angiography) study, CCTA, invasive angiography, and fractional flow reserve (FFR) were acquired for 383 lesions in patients with stable coronary syndromes [28]. The study revealed that LAP detected on CCTA significantly correlated with the presence of ischemia identified by FFR.

It has also been shown that the evaluation of plaque morphology with the detection of high-risk characteristics by CCTA is a useful method for forecasting future negative outcomes and the advancement of CAD. Motoyama et al., in a large longitudinal study, reported that both PR and LAP were strong predictors of future ACS events [29]. A sub-analysis of the SCOT-HEART trial revealed that the presence of adverse coronary plaque features confers a 3-fold increased risk of cardiovascular death or nonfatal MI [30]. Therefore, the Coronary Artery Disease Reporting and Data System (CAD-RADS) recommendations advise mentioning the existence of susceptible plaque whenever there are two or more high-risk criteria present (Figure 3) [31].

However, the image quality may be affected by artifacts invalidating the estimation of plaque morphology [32,33]. The most common are the motion and blooming artifacts, cause of severity overestimation of calcific plaques. The use of de-blooming algorithms and 3D reconstruction models allow us to overcome these limits ensuring a better CT-based analysis [34].

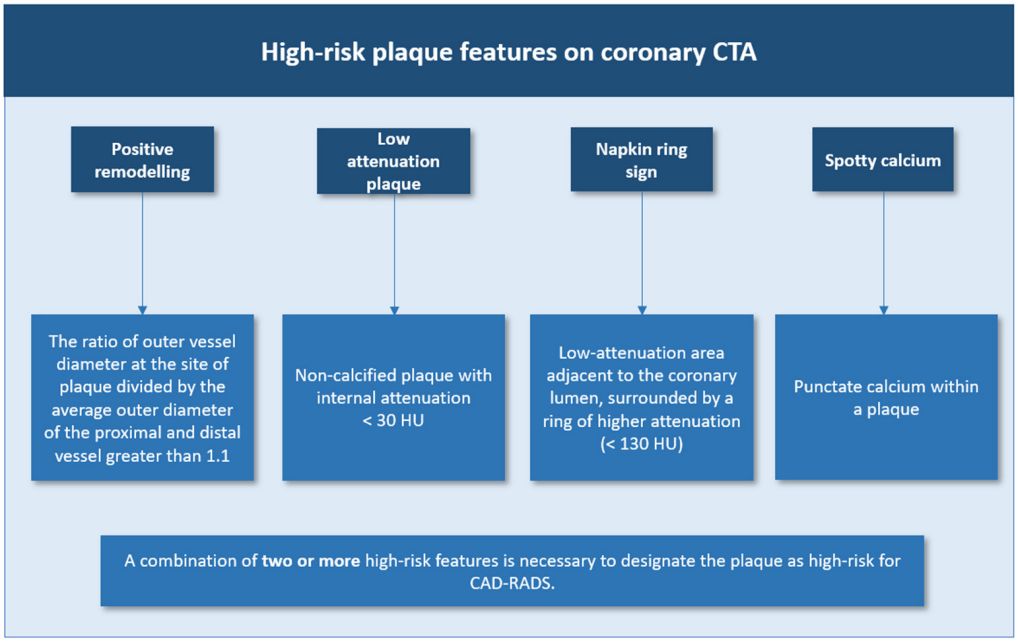

Figure 3. Vulnerable plaque features according to Coronary Artery Disease Reporting and Data System (CAD-RADS) guidelines.

1.5. CCTA in Previous Coronary Revascularization

The role of CCTA is still debated in patients previously revascularized with stents. The effectiveness of CCTA ≥64 slices for diagnosing coronary in-stent restenosis (ISR) and the effect of specific procedural aspects on diagnostic accuracy were examined in a recent meta-analysis that included 35 trials and 4131 stents [35]. This meta-analysis showed that CCTA could provide precise information about ISR lesions and that assessing these lesions could help identify changes over time. This is particularly important because patients with ISR may finally be suitable for non-invasive angiographic follow-up using CCTA. Nevertheless, in this context, CCTA has only been observed to have a high sensitivity in a few instances. For example, in stents with a diameter of >3 mm compared to those with lower diameters (94% vs. 89%), for stents with metal struts < 100 µm compared to thickening stents (96% vs. 84%), and for simple stents compared to stents implanted on bifurcations (95% vs. 88%) [19].

On the other hand, the role of CCTA in the evaluation of coronary artery bypass grafts (CABG) is more defined. A recent meta-analysis including 1975 patients and 5364 grafts revealed the excellent diagnostic performance of CCTA in the identification of graft stenosis or occlusion compared with invasive coronary angiography, with a sensitivity of 96%, a specificity of 96%, and a negative predictive value of 99% [36]. CCTA could also be used to assess the disease progression of native nongrafted vessels in patients with recurrent angina after CABG. Although these segments are often massively calcified and challenging to assess with CCTA, several studies, such as that of de Graaf et al., showed acceptable diagnostic accuracy for the detection of new coronary stenosis, with sensitivity and specificity of 83–100% and 77–100%, respectively [37].

2. Coronary Artery Calcium Score

To stratify cardiovascular risk, forecast patient outcomes, and direct preventative therapy, coronary artery calcium (CAC) scoring has become a widespread and efficient method. At this time, CAC score is advised to estimate the likelihood of developing cardiovascular diseases and mortality CAD-related in asymptomatic individuals [38]. Additionally, the CAC score is used to reclassify CV risk in other subgroups and to aid in developing primary prevention decisions such as statin therapy [19]. More recently, CT calcium scoring has become fundamental also in other clinical settings, such as allowing flow-independent

assessments of aortic stenosis severity when echocardiography measurements are discordant, pre-procedural planning of transcatheter aortic and mitral valve intervention, and in determining the etiology of cardiomyopathies [39].

2.1. Imaging Acquisition, Reconstruction, and Quantification of CAC

For CAC assessment, acquisition and reconstruction settings are standardized. Data are usually acquired using prospective electrocardiographic triggering in late diastole, with a section thickness of 2.5 mm, a section interval of 1 mm and without contrast material administration, using 120 kV tube voltage [38].

Electron-beam computed tomography (EBCT) and multi-detector computed tomography (MDCT) have been the main CT methods for CAC measurements, using fast scan speeds to reduce motion artifacts, with MDCT being associated with improved spatial resolution and largely replacing EBCT in practice [40].

Section thickness in the axial soft-tissue window and axial lung window settings for reconstruction is set to 2.5 mm. The CAC score is then determined using vendor-provided software, often measured with the use of the Agatston method, with calcification typically being defined as high attenuation (130 HU) and an area $\geq$ 1 mm [38,41]. The overall plaque area and a cofactor based on the attenuation of the plaque calcium in Hounsfield units are combined to get the Agatston score [38,42,43]. The area of the lesion (Ai) is multiplied by a weighting factor (wi) based on the maximal CT number (CTmax) in the segment of interest to determine the calcium score for each desired segment (CSi): CSi = wi x Ai, where wi is 1 if 130 HUCTmax <200 HU, 2 if 200 HU $\leq$ CTmax < 300 HU, 3 if 300 HU $\leq$ CTmax < 400 HU, 4 if 400 HU $\leq$ CTmax. Agatston score for each artery, each calcification, or the entire heart, also known as total calcium score (TCS), is calculated by summing the respective values for the regions of interest [41,43].

The Agatston score can be reported either as an absolute value with predetermined cut-offs or as a percentile compared to age-, sex-, and ethnicity-matched individuals using the Multi-Ethnic Study of Atherosclerosis (MESA) database [44]. As an alternative to total plaque burden, the following description of the total Agatston calcium score and the corresponding risk category is suitable: no coronary calcium, 1–9: minimal, 10–99: mild, 100–399: moderate, and $\geq$400: severe (Figure 4) [45]. However, the absolute measurement strategy outperformed the age-gender-ethnicity method, according to the MESA trial, even though both approaches produced effective risk categorization. In that study, even the lowest CAC (Agatston score of 1–10) was associated with a 3-fold increased risk of CAD than patients with an Agatston score of 0, and a score greater than 100 was associated with a 10-fold increased risk [44].

Another method for CAC assessment was developed based on volume scoring that represents the volume of the calcification; this score has become popular due to its relative resistance to slight variations in noise and its robust interscan reproducibility [46]. It is expressed with the product between the volume of one voxel and the number of voxels in the volume dataset related to the calcification. Nevertheless, there are several limits including the overestimation of the CAC grade in areas of strong attenuation and the vulnerability to partial volume averaging of this method. Another scoring system is the mass score, which is derived using the plaque volume, plaque attenuation, and a calibration factor that considers the water attenuation. Even though it is an up-and-coming method based on the measurement of a true mineral mass of calcium hydroxyapatite in the plaques, it requires complex postprocessing, and limited supporting data have been available so far [41,46]. Finally, Brown et al. proposed another score for clinical use, the calcium coverage score, defined as the percentage of coronary arteries affected by calcified plaque, which was highly associated with coronary heart disease events and provided information about cardiovascular occurrence beyond the calcium burden defined by the Agatston or calcium mass score [47].

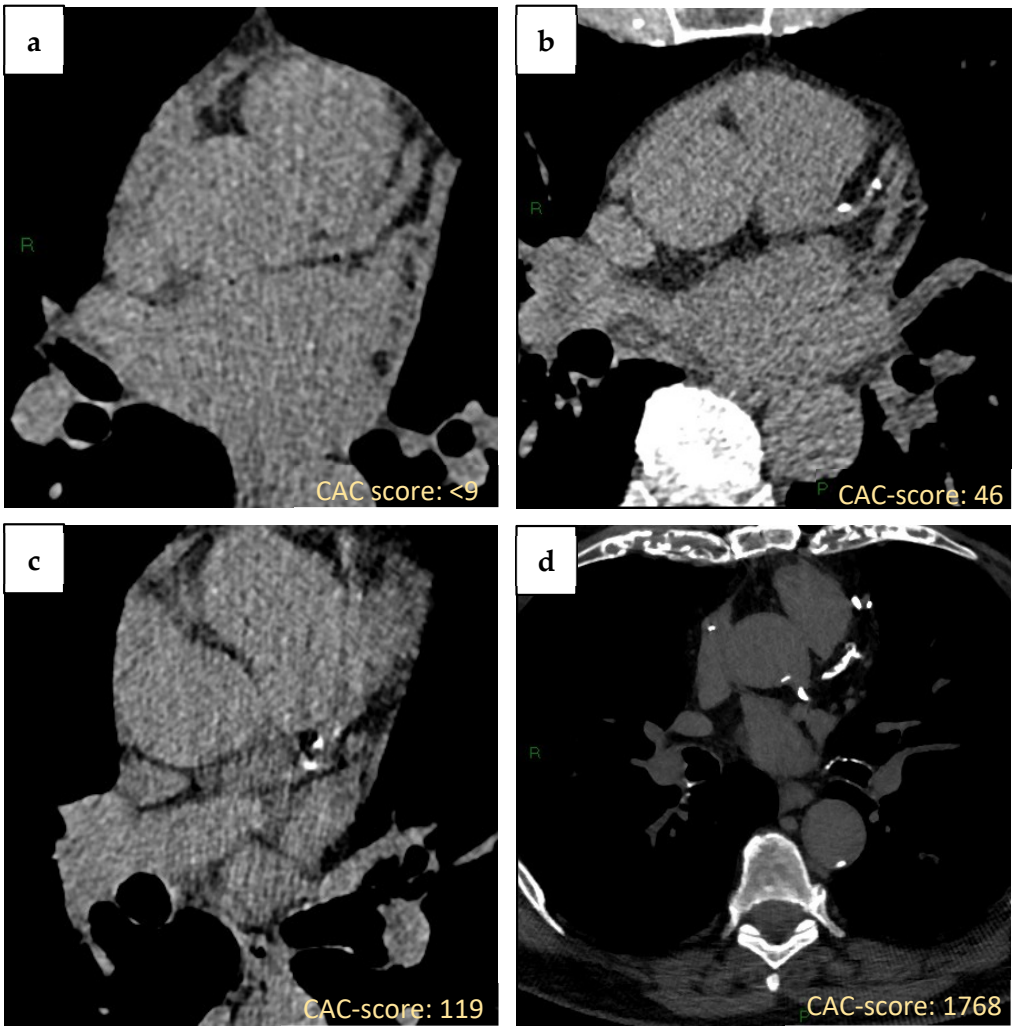

Figure 4. Coronary artery calcium (CAC) score assessment through cardiac computed tomography (CCT) stratified for risk category: (**a**) minimal risk, CAC score <9; (**b**) mild risk, CAC score 46; (**c**) moderate risk, CAC score 119; (**d**) severe risk, CAC score 1768.

2.2. Pathophysiological Mechanisms of Calcium Deposition

When foamy macrophages rich with lipids and vascular smooth muscle cells (VSMCs) start gathering in the coronary arteries, the atherosclerotic process begins. This provokes thickening of the tunica intima which is followed by an increase in free cholesterol, acellular remains and in the final stages of fibroatheroma, an almost total lack of extracellular matrix [48]. The earliest calcified components are made up of membrane-bound matrix vesicles that are actively calcifying, which are produced by apoptotic VSMCs [49]. Then, the coronary arteries calcification becomes an active pathogenic process, with ectopic bone production being the base of the process [50]. Notably, VSMCs usually express proteins that inhibit calcification. However, in the setting of atherosclerosis, the expression of some of these inhibitors (such as matrix Gla protein) is downregulated, contributing to a loss of homeostatic inhibition of calcification. On the other hand, transcription factors such as Msx2, Runx2, Sox9, Cbfa1, and bone morphogenetic proteins (BMPs) significantly increase the expression by VSMCs and macrophages of chondrocyte, osteoblastic, and osteoclastic-associated proteins facilitating the calcification process [51,52].

Only in histologic sections can these microcalcifications be identified, not with conventional imaging methods. When these minute calcium deposits consolidate, bigger calcium granules form that can be seen using common imaging methods such as CCTA. When macrocalcifications further aggregate, they could potentially form a large calcification

fragment that extends from the necrotic core to the collagen-rich matrix resulting in the formation of calcified plaque that may protrude into the lumen or media [48].

Inflammation, promoted by apolipoproteins and oxidized phospholipids in the artery wall, and oxidative stress are also essential in the vascular calcification process [53,54]. Furthermore, it has been estimated that conventional risk factors account for 40% of the variability of coronary calcification [55]. Indeed, CAC is strongly connected with low-density lipoprotein (LDL) cholesterol in young asymptomatic men [56]. Furthermore, glucose has been reported to promote vascular cell calcification, while insulin inhibits the same process [57]. In this regard, an increased coronary calcification has been demonstrated in diabetics, especially those with type II diabetes [58].

2.3. Prognostic Value of CAC and Risk Assessment

2.3.1. Asymptomatic Subjects

The most recent data suggest that, in addition to the established cardiac risk factors, the use of CAC is independently predictive of prognosis. Therefore, the rate of MACEs rises proportionally with increasing severity of coronary calcifications categorized by the Agatston calcium score [59,60]. While individuals with CAC levels $\geq$ 1000 have a mortality rate comparable to high-risk secondary prevention patients, asymptomatic subjects with 0 coronary calcium show a persistently very low risk throughout multiple studies [61,62].

CAC has also been demonstrated to further stratify patients who were assessed as intermediate risk using the Framingham Risk Score alone [63]. CAC score was independently predictive of ischemic outcomes above and beyond historical risk variables in univariable and multivariable models estimating CAD occurrence at 4.3 years of follow-up [64]. Other research has demonstrated that the incremental risk prediction value of CAC extended to both younger and older individuals, diabetic patients, smokers, and the elderly [65].

Furthermore, CAC may determine whether asymptomatic people might benefit from statin or aspirin as primary preventive therapy [66]. According to current recommendations for statin therapy, it is reasonable to assess CAC in patients with an intermediate risk of developing atherosclerotic cardiovascular disease [4]. However, none of the guidelines proposes management based on calcium score because of insufficient support from randomized clinical trials.

2.3.2. Symptomatic Patients

Recent European guidelines for the diagnosis and treatment of CCS state that CCTA is appropriate as a first-line diagnostic test for the evaluation of patients with no history of CAD, atypical or typical angina symptoms, or symptoms that are equivalent to angina, as well as patients who have undergone inconclusive stress testing. Three milestone multicenter studies which compared the accuracy of CCTA with ICA for the identification of obstructive coronary stenosis consistently reported high sensitivity values ranging from 85% to 95%, with a negative predictive value of almost 100% [67,68].

In this setting, CAC may raise estimates of the clinical likelihood of obstructive CAD (such as a coronary stenosis > 50%) together with sex, age, and symptoms. As a result of employing the CAC score in the pre-test estimate of the likelihood of CAD, more than half of symptomatic individuals were reclassified into a reduced risk category for obstructive CAD [69]. However, current evidence does not yet support its use as a diagnostic tool to rule out obstructive CAD because it does not provide precise information on the severity of coronary stenoses [8].

2.3.3. Role of CAC in Specific Subgroups

It is essential to mention the role of CCTA and CAC in some specific subgroups of patients at higher risk of developing ischemic events, such as those with diabetes, older age, and chronic renal insufficiency.

Patients with diabetes more frequently develop calcified and extensive CAD, presenting as silent ischemia, and greater plaque progression in terms of disease load and ad-

verse plaque characteristics than patients without diabetes. Therefore, Perrone-Filardi et al. reported higher mortality in diabetic patients than in nondiabetic patients for any degree of CAC [45]. Accordingly, a recent meta-analysis reported that the rise in CAC score is substantially linked to an elevated risk for all-cause mortality and/or fatal and non-fatal CV events in asymptomatic diabetics [70]. In addition, evaluation of CAC may help identify diabetic subjects who are more likely to have inducible ischemia and may be utilized as a strategy for preselecting people before functional imaging [45].

Few studies have examined the predictive significance of CAC in the elderly (>75 years). A recent study found that women are more at risk than men for cardiovascular and all-cause mortality, with CAC scores and percentiles being highly predictive of these outcomes among older persons. In contrast, relatively low-risk older individuals have low coronary artery calcium scores of 0 to 9 or 25th percentile [71].

Dialysis patients experience a faster progression of CAC, which is correlated with age, the length of dialysis, the etiology of chronic renal failure, changes in mineral metabolism, and the use and dosage of calcium-based phosphate binders. According to reports, the level of CAC in dialysis patients is related to cardiovascular outcomes [72]. However, further information is required to determine the potential practical application of the CAC score for further risk categorization of this subgroup [39].

2.3.4. CAC and Progression of Coronary Atherosclerosis

Calcium deposition within atherosclerotic plaques progresses by an average of 15 to 25% per year. Thus, the progression of CAC scores over time has been reported in several studies and associated with worse prognosis, as well as its regression due to specific anti-atherosclerotic therapies such as statins, has been associated with improved outcomes [44,73,74].

Previous studies have shown that CAC progression has been associated with a higher risk for MI and all-cause mortality [75–77]. Conversely, the Cooper Center Longitudinal Study (CCLS trial) found no additional predictive value of CAC progression compared with the single CAC measurement on cardiovascular outcomes [77]. Likewise, Lehmann et al. observed that CAC progression adds only weakly to risk prediction models for CAD, solely for those patients reporting a significant increase in CAC between baseline and 5-year follow-up (from 1 to 399 to CAC $\geq$ 400), who demonstrated a nearly 2-fold increase in cardiovascular events than subjects in which CAC remained below 400 [78]. Therefore, a second CAC scan may be beneficial in the presence of CAC > 0 to determine if and when CAC values tend to exceed the high-risk threshold of CAC $\geq$ 400 [78].

2.4. Emerging Technologies

Different technologies are emerging to overcome CAC's current limitations and offer better tools and methods for clinical decision-making. CAC scoring non-gated CT scans, dual-energy CT and virtual non-contrast imaging, and artificial intelligence for automatic CAC scoring show great potential [38]. Regarding non-gated-CT scan, the 2016 Society of Cardiovascular Computed Tomography (SCCT) and the Society of Thoracic Radiology (STR) guidelines recommended its use in the evaluation of CAC even in patients without known CAD for better prognostic stratification [79]. Furthermore, CT-derived FFR has been shown, together with other CT-derived hemodynamic parameters (wall shear stress and axial plaque stress) [80], to improve the specificity and accuracy of CCTA in several clinical trials, especially when assessing intermediate stenoses and may improve the selection of patients who are most likely to benefit from coronary angiography and revascularization [81]. On the other hand, computed tomography perfusion (CTP) imaging may be useful when the value of FFR is in the gray area (for example, 0.74–0.85) or when FFR cannot be calculated due to technical reasons. They allow to integrate the morphological data with hemodynamic risk indexes leading to better plaque evaluation. Integrating these analyses also with ECG-derived electromechanical parameters able to predict myocardial ischemia, we could

get complex models based on multimodal data analysis achieving a patient-specific risk assessment [82–84].

The combination with electromechanical models [85] could allow to overcome the limit of the CT-derived FFR overestimation in patients with concomitant coronary microvascular dysfunction, improving diagnostic accuracy [86–88].

Furthermore, integrating anatomical and functional imaging or hybrid imaging such as single positron emission computed tomography (SPECT)/CCTA may improve the selection of candidates for invasive procedures in patients with uncertain results with one of the two techniques [89].

However, further studies are requested to obtain strong evidence about the cost-effectiveness, the prognostic value of these technologies and their role in clinical decision-making [19,90].

3. Epicardial Adipose Tissue

The epicardial adipose tissue (EAT) is a metabolically active organ recently associated with heart failure and atrial fibrillation and classified as an independent risk factor for subclinical coronary artery disease [91,92]. For this reason, in the last years, some evidence suggests as the assessment of EAT using CCTA might represent an additional tool to quantify patients' cardiovascular risk.

3.1. Anatomy and Functions of Epicardial Adipose Tissue

The intrathoracic adipose tissue surrounding the heart can be divided into epicardial adipose tissue (EAT) and pericardial fat (PF). The PF is located between the pericardial visceral and parietal layers; it derives from the primitive thoracic mesenchyme and is supplied by branches of the internal thoracic artery [93]. On the other hand, EAT is placed between the pericardial visceral layer and the myocardial muscle covering about 80% of the cardiac surface; it originates from the splanchnopleuric mesoderm and is vascularized by branches of coronary arteries. Lastly, the portion of the EAT immediately contiguous with the adventitial layer of coronary arteries is called pericoronary adipose tissue (PCAT) [94].

The EAT is microscopically composed of different cells, including adipocytes, resident monocytes, immune cells, and nerve cells [95]. Interestingly, no muscle fascia between EAT and myocardium is present, allowing direct communication between these two organs through paracrine and vasocrine mechanisms [93]. Physiologically, EAT plays a protective role for the heart. It acts as a local energy store and provides free fatty acids to the myocardial tissue in times of high demand [96]. It also releases adipokines with anti-inflammatory, antioxidant, and vasodilator functions (adiponectin and adrenomedullin) [97]. In addition, the EAT offers mechanical support preventing coronary artery torsion during cardiac contraction, exerts a thermoregulatory function [96] and acts as an immune organ [98].

However, in pathological conditions, EAT becomes pro-arrhythmogenic and pro-atherogenic. Indeed, in patients who have CAD, EAT shows pro-inflammatory features with an increased concentration of inflammatory M1 macrophages than anti-inflammatory M2 macrophages [99], higher production of interleukin-6 (IL-6), interleukin-1 (IL-1), and tumor necrosis factor-alpha (TNF-a) associated with reduced production of adiponectin and adrenomedullin, and an elevated concentration of reactive oxygen species (ROS) [100].

The mechanisms of EAT dysfunction might translate into atherosclerotic plaque development are not entirely known. However, it has been proposed that macrophages, together with T- and B-lymphocytes, are triggered by the Toll-like receptor (TLR) binding that stimulates nuclear factor-κB (NF-κB) and JUNN-terminal kinase (JNK) [101,102]. The activation of these two molecules leads to increased interleukin production, such as IL-6, facilitating endothelial cell permeability and monocyte adhesion [103]. The entire process is powered by the increased ROS levels that further favor endothelial dysfunction and interleukin secretion [100].

3.2. Quantification of Epicardial Adipose Tissue Using CCTA

A trustworthy quantification of EAT can be obtained using different non-invasive techniques. EAT thickness could be measured by transthoracic echocardiography on the free wall of the right ventricle [104]. However, CCTA is considered the most validated and reproducible technique for its quantification, given the higher spatial resolution compared to magnetic resonance (MR) and allowing for simultaneous evaluation of CAD [105].

In detail, quantification of EAT by CCTA envisages the measure of density (Hounsfield units), volume (cm^3), and thickness (mm). Epicardial fat density ranges from −190 to −30 Hounsfield units (HU) [106]. Measurements of thickness may be achieved in the horizontal long-axis plane, in the basal short-axis plane, and over the right ventricular free wall [107]. Regarding volume quantification, manual segmentation of EAT is the most widespread method. The operator manually draws EAT contours every 15 mm within a region of interest that usually includes the anterosuperior mediastinum at the pulmonary trunk level, the left main trunk, the left anterior descending and circumflex arteries in proximal segments, the posterior mediastinum, and the inferior diaphragmatic surface. (Figure 5a–c) Different software can be used to optimize and speed up this process [108]. The advantages of CT volumetric quantification are the high definition and reproducibility, whereas the main limitation is the need for a long segmentation time for an accurate measurement [109]. EAT can also be measured during coronary CT in the interval between contrast administration and angiographic acquisition and does not require specific acquisition [108].

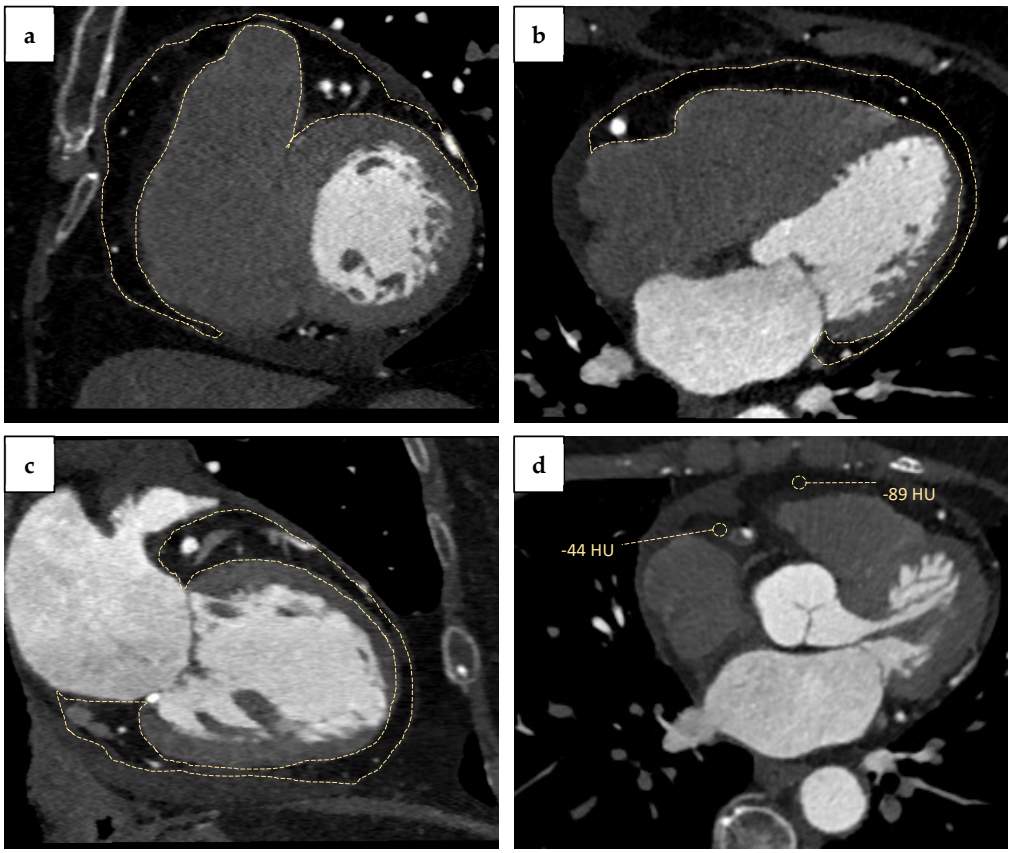

Figure 5. Cardiac computed tomography angiography (CCTA) assessment of epicardial adipose tissue (EAT) and peri-coronary adipose tissue (PCAT): (**a**) EAT in short-axis view; (**b**) EAT in four-chamber view; (**c**) EAT in two-chamber view (dashed line); (**d**) peri-coronary adipose tissue (PCAT) radiodensity (−44 HU) compared with radiodensity of EAT surrounding free left ventricle wall (−89 HU).

3.3. Epicardial Fat Volume and Atherosclerosis Progression

Recent studies have demonstrated that EAT volume is associated with the development and progression of atherosclerotic plaques. Therefore, previous studies reported greater EAT volumes in patients with angiographic evidence of coronary stenoses than those without [110,111]. Similarly, Gitsioudis et al., enrolling patients with intermediate CAD risk undergoing cardiac CT with contextual EAT volume quantification, showed a higher EAT volume in patients with coronary stenosis >50% compared with those with <50%. Moreover, the multivariate regression analysis revealed an independent association between coronary stenosis severity, plaque burden, and EAT volume [112].

Notably, EAT volume is also associated with atherosclerosis progression and, more specifically, with the development of high-risk plaques. In this regard, Alexopoulos et al. demonstrated that EAT was higher in patients with mixed/non-calcified plaques than those with calcified lesions [113]. The same evidence was reported by Tsuyoshi et al., that quantified epicardial fat volume in 1308 patients with symptomatic CAD and a zero-calcium score. EAT was greater in patients with obstructive atherosclerotic plaques than no plaque and even more in those with vulnerable plaque than no plaque [114]. Similarly, a recent meta-analysis by Nerlekar et al. confirmed the association between EAT volume and high-risk plaques [115]. Otsuka et al. found that EAT volume in ACS patients was significantly higher than in those suffering from CCS [116]. Finally, Yamashita et al. demonstrated a significant positive correlation between EAT volume and necrotic plaque detected using intravascular ultrasound imaging (IVUS) and a negative correlation between EAT volume and fibrous plaque [117].

Several studies also reported a direct relationship between EAT and CAC score. Iwasaki et al. demonstrated increased CAC in patients with EAT volume >100 cm^3 than in those with EAT volume <100 cm^3, with a higher incidence of CAD in the same group [118]. These results were confirmed in the study conducted by Cosson et al., where EAT volume was independently associated with CAC $\geq$ 100 AU (per 10 cm^3 increase: OR 1.11 (1.02–1.20)) [119].

Another measurable parameter derived from EAT assessment and associated with a worse prognosis is fat radiodensity. Franssens et al. demonstrated in 140 patients undergoing CT-scan that one standard deviation lower EAT attenuation (5 HU) was associated with 1.9 and 1.07 higher odds (for men and women respectively) of being in higher CAC class (0, 1 to 100, 101 to 400, and >400) [120]. Similarly, Goeller et al. quantified both EAT volume and density in 456 asymptomatic patients; EAT volume resulted lowest in patients without coronary calcium and higher in patients with severe atherosclerosis, while EAT density resulted lower in patients with high coronary calcium and increased occurrence of adverse clinical events [121].

Finally, all this evidence allows identifying EAT volume as a predictor of MACEs. For example, Eisenberg et al. quantify EAT volume in asymptomatic patients from the EISNER (Early Identification of Subclinical Atherosclerosis by Noninvasive Imaging Research) trial, showing its association with increased risk of MACE after 14 $\pm$ 3 years of follow-up. It was also demonstrated that MACE risk progressively increased with EAT volume $\geq$ 113 cm^3 and CAC $\geq$ 100 AU [122]. Thus, Fuller et al. revealed that patients with CAD who died from sudden cardiac death had significantly higher EAT thickness [123]. Moreover, in the Heinz Nixdorf Recall Study, the incidence of coronary events increased directly with EAT quartiles, with a doubling of EAT volume associated with a 1.5-fold risk of coronary events independently from other traditional CV risk factors [124].

3.4. Pericoronary Fat: Marker of Coronary Artery Stenosis Severity

Another CT-measurable parameter associated with CAD severity is the pericoronary fat (Figure 5d). In this regard, a study conducted by Gorter et al. evaluated in 128 symptomatic patients undergoing percutaneous coronary intervention (PCI) the EAT volume and the pericoronary fat. Patients with low BMI and multivessel coronary disease had increased values of both CT parameters compared to patients without CAD [125]. Likewise, Balcer

et al. analyzed PCAT volume in 46 patients with acute MI undergoing coronary-CT angiography, demonstrating higher values around culprit lesions than non-culprit ones [126]. Furthermore, Ma et al. reported a raised pericoronary adipose tissue mean attenuation (PCATMA) in arteries with CT-measured plaques, particularly in non-calcified/mixed plaques [127]. Interestingly, PCATMA was also associated with in-stent restenosis. Thus, Nogic et al. enrolled 151 patients undergoing CT-scan for suspected CAD, treated with stent implantation within three months and that repeated coronary angiography after a maximum of five years for any reason. The study demonstrated that patients with ISR had a significantly increased lesion-specific PCATMA at baseline compared with patients without stent hyperplasia [128].

3.5. Effective Therapies in the Reduction of Epicardial Fat

Recent studies have shown several drugs' efficacy in reducing EAT thickness and volume. Thanks to their pleiotropic effects, statins have been reported to reduce epicardial fat metabolic activity, thickness, and attenuation [129]. In this setting, atorvastatin provided better results than pravastatin [130]. Furthermore, metformin also reduced EAT thickness after three months of treatment in diabetic patients [131]; similar results were reported for liraglutide, semaglutide, and dulaglutide [132,133]. Correspondingly, sodium-glucose cotransporter 2 (SGLT-2) inhibitors (dapagliflozin and empagliflozin) demonstrated a reduced EAT volume in CAD patients after six months of treatment [134]. Notwithstanding, further studies are needed to evaluate how the well-known cardiovascular benefit of all these drugs might be related to the attenuation of EAT thickness and volume.

4. Additional CT-Measurable Parameters for Cardiovascular Risk Stratification

4.1. Aortic Calcium

The assessment of extra coronary calcifications, such as aortic valve calcification, mitral annular calcification, and thoracic aortic calcium (TAC), can improve cardiovascular risk stratification beyond the CAC score. Notably, non-contrast cardiac CT estimates coronary and extra coronary calcifications with the same scans without additional scanning or radiation.

Different methods for evaluating TAC have been reported. The simplest one is just identifying the presence or absence of aortic calcium, recording TAC in a binary fashion. Alternatively, TAC can be expressed with the Agatston method, similar to CAC [135]. Several studies demonstrated a correlation between TAC and cardiovascular events. In the Multi-Ethnic Study of Atherosclerosis (MESA), Budoff et al. demonstrated that TAC predicted future cardiovascular events over risk factors and CAC, but only in women [136]. Another study by Santos et al. showed that the presence of TAC was associated with all-cause mortality. This relationship was independent of conventional cardiovascular risk factors and the presence of CAC. Accordingly, Allison et al. showed that multisite calcifications, including thoracic aortic calcifications, predict total mortality [137].

Furthermore, previous studies have reported a close relationship between TAC and CAC. Rivera et al. analyzed a cohort from the MESA and demonstrated that TAC is significantly associated with CAC incidence and progression [138]. Previously, Kuller and colleagues showed that the presence of TAC and carotid plaques in postmenopausal women is significantly related to CAC [139].

4.2. Liver Fat

Cardiac CT scans used for CAC scoring can also identify both epicardial and liver fat (LF) without any modifications to the scan protocol; this latter is identified as a decreased liver attenuation [140]. The attenuation measurement obtained with CT is more reliable than that obtained with echocardiography or cardiac magnetic resonance (CMR), especially in a homogeneous and non-hypervascular parenchymal organ [141]. Cardiac CT generally does not include the whole liver in the scans. However, it has been demonstrated that

the attenuation measurement of two or three sites of the liver reflects that of the whole liver [142].

LF is considered a marker of cardio-metabolic health because it is closely associated with non-alcoholic fatty liver disease (NAFLD), which is correlated to metabolic syndrome and CV disease [143,144]. Indeed, it has been shown that patients with NAFLD have an increased risk of developing atherosclerotic disease [144]. In this regard, NAFLD has been independently associated with increased carotid intima-media thickness (CIMT) and CAC, both measures of atherosclerosis severity [145]. In addition, the ROMICAT II trial demonstrated that high-risk plaque features evaluated by CCTA (positive remodeling, napkin-ring sign, spotty calcification, low attenuation) were more frequent in patients with NAFLD compared with patients without NAFLD [146]. Furthermore, Wolff et al. investigated the relationship between LF, traditional cardiovascular risk factors and subclinical coronary artery disease [147]. The authors found that LF was associated with all traditional cardiovascular risk factors, specifically to waist circumference, diastolic blood pressure, HDL cholesterol and diabetes mellitus. Additionally, a greater volume of LF was associated with a higher burden of subclinical CAD, regardless of the presence of other cardiovascular risk factors [147].

Several mechanisms have been proposed to motivate the relationship between LF and CAD. Firstly, the fatty liver excretes high levels of substances that damage the cardiovascular system, such as coagulation factors, very low-density lipoproteins, and C-reactive protein. Additionally, LF is closely linked to insulin resistance and pro-inflammatory status [148,149]. All this evidence suggests that LF, measured with CT, can be valid for a comprehensive cardiovascular risk assessment together with other CT parameters.

4.3. Myocardial Scar

An emerging application of non-contrast cardiac CT in detecting myocardial scars due to an occult MI has recently been demonstrated. The 10-year mortality related to unrecognized MI is estimated to be 45–50% [150]. Therefore, recognizing occult MI is crucial to identify that subgroup of patients who could benefit from intensive medical treatments, coronary revascularization procedures, or implantable cardioverter defibrillator implantation. The evidence of an occult MI also has prognostic value since it is considered a predictor of MACE recurrence and cardiac death.

The areas of old MI appear hypo-attenuated due to fatty replacement on non-contrast cardiac CT or pre-contrast cardiac CT [151]. Specifically, myocardial fat associated with an old MI appears on CT as an area of subendocardial hypoattenuation following the culprit coronary artery [152,153]. In this regard, Ichikawa et al. showed that left ventricle myocardial fat can be observed at least after three years from the MI with a subendocardial location [154]. Furthermore, in patients with old MI the different CT attenuation between normal and necrotic myocardium is more significant compared to patients with acute MI, suggesting that cardiac CT may help differentiate between recent and old MI [155]. Another interesting study evaluated the ability of non-contrast cardiac CT to identify chronic MI in patients with evidence of no-reversible perfusion alterations on nuclear myocardial imaging [156]. Sixty-two patients with non-reversible perfusion defects underwent CAC scanning and MI was identified as a hypo-attenuation area on CT. The study showed that non-contrast cardiac CT was able to identify prior MI in 57 patients, with a sensitivity of 92% [156].

Furthermore, the delayed enhancement cardiac CT, which shares a similar pathophysiological basis with delayed enhancement cardiac magnetic resonance, provides more specific information in this context. A delayed phase CT scan is generally performed 5–15 min after CCTA with the administration of an additional contrast medium. Iodinated contrast is an extracellular contrast agent with late washout from areas of abnormal myocardium, such as fibrosis or scar [157]. Therefore, cardiac CT with delayed enhancement can be used to identify myocardial scar or fibrosis in both ischemic and non-ischemic cardiopathy, similar to CMR with late gadolinium enhancement, which is actually the

gold standard for tissue characterization. Compared with CMR, cardiac CT has some advantages, such as higher availability and shorter examination time. It can also be helpful in patients with CMR contraindications (i.e., claustrophobia and metallic implants).

Several studies demonstrated that contrast-enhanced cardiac CT allows the identification and quantification of MI, showing a good agreement with CMR [158–160]. Specifically, two different contrast-enhancement patterns can be observed in case of MI: early hypo-enhancement, which is correlated to the microvascular obstruction in acute MI, and delayed hyper-enhancement, which is typical of chronic MI. Therefore, the ability of cardiac CT to characterize ischemic myocardium can be helpful in the clinical reality to stratify cardiovascular risk and also to manage clinical decisions. In addition, delayed enhancement cardiac CT may facilitate, in patients with acute chest pain and elevated cardiac biomarkers, the differentiation of myocarditis and ACS through the detection of the characteristic mid-wall or subepicardial delayed enhancement and the absence of significant coronary stenosis in patients with myocarditis. Indeed, Palmisano et al. demonstrated in patients with acute chest pain and elevated cardiac troponin with negative triple rule out (TRO) CT scan that late contrast enhancement CT can increase the diagnostic rate identifying myocarditis, myocardial infarction with non-obstructed coronary artery (MINOCA) and Takotsubo cardiomyopathy [161].

For instance, Bouleti et al. demonstrated that delayed phase cardiac CT could be a valid alternative to delayed enhancement CMR in detecting inflammatory segments in patients with acute myocarditis, with a diagnostic accuracy of 95% [162]. Furthermore, Esposito et al. showed that cardiac CT with delayed enhancement also provides a three-dimensional characterization of myocardial scars associated with ventricular tachycardias. This information may help to plan electrophysiological procedures such as electro-anatomic mapping and arrhythmias radiofrequency catheter ablation [163].

Lastly, delayed enhancement cardiac CT can be used to measure an index of diffuse myocardial fibrosis, which is named myocardial extracellular volume fraction (ECV) [164]. ECV can be estimated using the following method obtained from cardiac CT: ECV = (1–hematocrit) × (ΔHULV myocardium/ΔHULV blood), where ΔHU is the change in HU attenuation pre-contrast and in the delayed phase CT (HU delayed phase – HU pre-contrast) [157]. The measurement of ECV with cardiac CT can be helpful in the setting of non-ischemic cardiomyopathies, such as hypertrophic cardiomyopathy, cardiac amyloidosis, dilated cardiomyopathy, and sarcoidosis. Hence, several studies demonstrated that mean ECV values obtained with delayed phase cardiac CT are significantly higher in patients with hypertrophic cardiomyopathy, cardiac amyloidosis and dilated cardiomyopathy compared to healthy subjects [165,166]. In these patients, delayed enhancement cardiac CT also assesses the identification of myocardial fibrosis areas with various delayed enhancement patterns (transmural, subepicardial, subendocardial, or mid myocardial).

5. Limits of CCTA

There are several limits of the CCTA. Respiratory motion artifacts are a frequent issue in image acquisition that can reduce image quality. The presence of arrhythmias or other technological factors might also cause problems with electrocardiographic gating during picture acquisition. In some cases, there may be technical problems such as partial exclusion of the coronary arteries from the field of vision [41,90]. Besides that, coronary artery motion artifacts, non-coronary calcium (for instance calcified thoracic lymph nodes, pleural or pericardial calcifications, mitral annular calcification), and artifacts from adjacent metallic prostheses are potential issues that can cause CAC calculation and other CT parameters assessment to be inaccurate [38]. Moreover, radiation exposure is also a limiting factor. However, radiation doses may be further reduced using low tube potential (<100 kVp) and high-pitch helical acquisition, when appropriate, and consequent heart rate lowering [167].

6. Conclusions

CCTA is a first-line investigation tool approved by the current AHA and ESC guidelines for detecting coronary stenosis in chronic and acute coronary syndromes [6,8]. Moreover, through CAC scoring assessment, it is also recommended in asymptomatic patients for cardiovascular risk stratification [4]. Recently, CCTA's role as a predictor of plaque burden has been emerging, and other measurable parameters are being evaluated. Beyond CAC, EAT volume is the more promising, associated with atherosclerosis progression, development of high-risk plaques, and increased MACEs [110–123]. The others are aortic calcium [137] (able to improve CV risk stratification exceeding CAC score), liver fat [144] (a marker of cardio-metabolic health and atherosclerosis development) and myocardial scar [155] (an indicator of worst prognosis in patients with myocardial infarction). In the future, these novel CCTA applications allow a better prognostic stratification and early detection of patients at risk of developing severe atherosclerosis and adverse clinical events. Notwithstanding the need for further studies, their use in clinical practice might also guide optimal primary and secondary prevention strategies.

Author Contributions: Conceptualization, A.N. and F.B.; validation, F.G. and G.P.U.; writing, A.N., F.B., F.C., M.G. and M.C.; review and editing, A.N., N.C., R.R. and D.D.S.; visualization, F.P., F.M., P.G. and V.C.; supervision, F.G., G.P.U. and C.C.Q. All authors have read and agreed to the published version of the manuscript.

Funding: This research received no external funding.

Conflicts of Interest: The authors declare no conflict of interest.

References

1. Ralapanawa, U.; Sivakanesan, R. Epidemiology and the Magnitude of Coronary Artery Disease and Acute Coronary Syndrome: A Narrative Review. *J. Epidemiol. Glob. Health* **2021**, *11*, 169–177. [CrossRef] [PubMed]
2. Mach, F.; Baigent, C.; Catapano, A.L.; Koskinas, K.C.; Casula, M.; Badimon, L.; Chapman, M.J.; De Backer, G.G.; Delgado, V.; Ference, B.A.; et al. 2019 ESC/EAS Guidelines for the Management of Dyslipidaemias: Lipid Modification to Reduce Cardiovascular Risk. *Eur. Heart J.* **2020**, *41*, 111–188. [CrossRef] [PubMed]
3. Liew, S.M.; Lee, W.K.; Khoo, E.M.; Ismail, I.Z.; Ambigapathy, S.; Omar, M.; Suleiman, S.Z.; Saaban, J.; Mohd Zaidi, N.F.; Yusoff, H. Can Doctors and Patients Correctly Estimate Cardiovascular Risk? A Cross-Sectional Study in Primary Care. *BMJ Open* **2018**, *8*, e017711. [CrossRef]
4. Visseren, F.L.J.; Mach, F.; Smulders, Y.M.; Carballo, D.; Koskinas, K.C.; Bäck, M.; Benetos, A.; Biffi, A.; Boavida, J.-M.; Capodanno, D.; et al. 2021 ESC Guidelines on Cardiovascular Disease Prevention in Clinical Practice. *Eur. Heart J.* **2021**, *42*, 3227–3337. [CrossRef] [PubMed]
5. Volume-, J.E. New Insights in Cardiovascular Risk Estimation and Stratification. *e-J. Cardiol. Pract.* **2022**, *22*, 1–9.
6. Fihn, S.D.; Gardin, J.M.; Abrams, J.; Berra, K.; Blankenship, J.C.; Dallas, A.P.; Douglas, P.S.; Foody, J.M.; Gerber, T.C.; Hinderliter, A.L.; et al. 2012 ACCF/AHA/ACP/AATS/PCNA/SCAI/STS Guideline for the Diagnosis and Management of Patients with Stable Ischemic Heart Disease. *Circulation* **2012**, *126*, e354–e471. [CrossRef]
7. National Institute for Health and Care Excellence (NICE). *Putting NICE Guidance into Practice Resource Impact Report: Hypercholesterolaemia and Mixed*; National Institute for Health and Care Excellence (NICE): London, UK, 2016.
8. Knuuti, J.; Wijns, W.; Saraste, A.; Capodanno, D.; Barbato, E.; Funck-Brentano, C.; Prescott, E.; Storey, R.F.; Deaton, C.; Cuisset, T.; et al. 2019 ESC Guidelines for the Diagnosis and Management of Chronic Coronary Syndromes. *Eur. Heart J.* **2020**, *41*, 407–477. [CrossRef]
9. Douglas, P.S.; Hoffmann, U.; Patel, M.R.; Mark, D.B.; Al-Khalidi, H.R.; Cavanaugh, B.; Cole, J.; Dolor, R.J.; Fordyce, C.B.; Huang, M.; et al. Outcomes of Anatomical versus Functional Testing for Coronary Artery Disease. *N. Engl. J. Med.* **2015**, *372*, 1291–1300. [CrossRef]
10. The SCOT-HEART Investigators. Coronary CT Angiography and 5-Year Risk of Myocardial Infarction. *N. Engl. J. Med.* **2018**, *379*, 924–933. [CrossRef]
11. Amsterdam, E.A.; Wenger, N.K.; Brindis, R.G.; Casey, D.E.; Ganiats, T.G.; Holmes, D.R.; Jaffe, A.S.; Jneid, H.; Kelly, R.F.; Kontos, M.C.; et al. 2014 AHA/ACC Guideline for the Management of Patients with Non–ST-Elevation Acute Coronary Syndromes. *J. Am. Coll. Cardiol.* **2014**, *64*, e139–e228. [CrossRef]

12. Collet, J.-P.; Thiele, H.; Barbato, E.; Barthélémy, O.; Bauersachs, J.; Bhatt, D.L.; Dendale, P.; Dorobantu, M.; Edvardsen, T.; Folliguet, T.; et al. 2020 ESC Guidelines for the Management of Acute Coronary Syndromes in Patients Presenting without Persistent ST-Segment Elevation. *Eur. Heart J.* **2021**, *42*, 1289–1367. [CrossRef] [PubMed]
13. Hadamitzky, M.; Distler, R.; Meyer, T.; Hein, F.; Kastrati, A.; Martinoff, S.; Schömig, A.; Hausleiter, J. Prognostic Value of Coronary Computed Tomographic Angiography in Comparison with Calcium Scoring and Clinical Risk Scores. *Circ. Cardiovasc. Imaging* **2011**, *4*, 16–23. [CrossRef] [PubMed]
14. Andreini, D.; Pontone, G.; Mushtaq, S.; Bartorelli, A.L.; Bertella, E.; Antonioli, L.; Formenti, A.; Cortinovis, S.; Veglia, F.; Annoni, A.; et al. A Long-Term Prognostic Value of Coronary CT Angiography in Suspected Coronary Artery Disease. *JACC Cardiovasc. Imaging* **2012**, *5*, 690–701. [CrossRef] [PubMed]
15. Finck, T.; Hardenberg, J.; Will, A.; Hendrich, E.; Haller, B.; Martinoff, S.; Hausleiter, J.; Hadamitzky, M. 10-Year Follow-Up after Coronary Computed Tomography Angiography in Patients with Suspected Coronary Artery Disease. *JACC Cardiovasc. Imaging* **2019**, *12*, 1330–1338. [CrossRef] [PubMed]
16. Al-Mallah, M.H.; Qureshi, W.; Lin, F.Y.; Achenbach, S.; Berman, D.S.; Budoff, M.J.; Callister, T.Q.; Chang, H.-J.; Cademartiri, F.; Chinnaiyan, K.; et al. Does Coronary CT Angiography Improve Risk Stratification over Coronary Calcium Scoring in Symptomatic Patients with Suspected Coronary Artery Disease? Results from the Prospective Multicenter International CONFIRM Registry. *Eur. Heart J.—Cardiovasc. Imaging* **2014**, *15*, 267–274. [CrossRef]
17. Bittencourt, M.S.; Hulten, E.; Ghoshhajra, B.; O'Leary, D.; Christman, M.P.; Montana, P.; Truong, Q.A.; Steigner, M.; Murthy, V.L.; Rybicki, F.J.; et al. Prognostic Value of Nonobstructive and Obstructive Coronary Artery Disease Detected by Coronary Computed Tomography Angiography to Identify Cardiovascular Events. *Circ. Cardiovasc. Imaging* **2014**, *7*, 282–291. [CrossRef]
18. Hadamitzky, M.; Taubert, S.; Deseive, S.; Byrne, R.A.; Martinoff, S.; Schomig, A.; Hausleiter, J. Prognostic Value of Coronary Computed Tomography Angiography during 5 Years of Follow-up in Patients with Suspected Coronary Artery Disease. *Eur. Heart J.* **2013**, *34*, 3277–3285. [CrossRef]
19. Pontone, G.; Rossi, A.; Guglielmo, M.; Dweck, M.R.; Gaemperli, O.; Nieman, K.; Pugliese, F.; Maurovich-Horvat, P.; Gimelli, A.; Cosyns, B.; et al. Clinical Applications of Cardiac Computed Tomography: A Consensus Paper of the European Association of Cardiovascular Imaging—Part I. *Eur. Heart J.—Cardiovasc. Imaging* **2022**, *23*, 299–314. [CrossRef]
20. Weir-McCall, J.R.; Villines, T.C.; Shaw, L.J.; Abbara, S.; Ferencik, M.; Nieman, K.; Achenbach, S.; Nicol, E. Highlights of the Twelfth Annual Scientific Meeting of the Society of Cardiovascular Computed Tomography. *J. Cardiovasc. Comput. Tomogr.* **2018**, *12*, 3–7. [CrossRef]
21. Min, J.K.; Shaw, L.J.; Devereux, R.B.; Okin, P.M.; Weinsaft, J.W.; Russo, D.J.; Lippolis, N.J.; Berman, D.S.; Callister, T.Q. Prognostic Value of Multidetector Coronary Computed Tomographic Angiography for Prediction of All-Cause Mortality. *J. Am. Coll. Cardiol.* **2007**, *50*, 1161–1170. [CrossRef]
22. Lee, S.-E.; Chang, H.-J.; Sung, J.M.; Park, H.-B.; Heo, R.; Rizvi, A.; Lin, F.Y.; Kumar, A.; Hadamitzky, M.; Kim, Y.J.; et al. Effects of Statins on Coronary Atherosclerotic Plaques. *JACC Cardiovasc. Imaging* **2018**, *11*, 1475–1484. [CrossRef] [PubMed]
23. Chang, H.-J.; Lin, F.Y.; Lee, S.-E.; Andreini, D.; Bax, J.; Cademartiri, F.; Chinnaiyan, K.; Chow, B.J.W.; Conte, E.; Cury, R.C.; et al. Coronary Atherosclerotic Precursors of Acute Coronary Syndromes. *J. Am. Coll. Cardiol.* **2018**, *71*, 2511–2522. [CrossRef] [PubMed]
24. Maurovich-Horvat, P.; Hoffmann, U.; Vorpahl, M.; Nakano, M.; Virmani, R.; Alkadhi, H. The Napkin-Ring Sign: CT Signature of High-Risk Coronary Plaques? *JACC Cardiovasc. Imaging* **2010**, *3*, 440–444. [CrossRef] [PubMed]
25. Maurovich-Horvat, P.; Schlett, C.L.; Alkadhi, H.; Nakano, M.; Otsuka, F.; Stolzmann, P.; Scheffel, H.; Ferencik, M.; Kriegel, M.F.; Seifarth, H.; et al. The Napkin-Ring Sign Indicates Advanced Atherosclerotic Lesions in Coronary CT Angiography. *JACC Cardiovasc. Imaging* **2012**, *5*, 1243–1252. [CrossRef] [PubMed]
26. Nakazato, R.; Otake, H.; Konishi, A.; Iwasaki, M.; Koo, B.-K.; Fukuya, H.; Shinke, T.; Hirata, K.-i.; Leipsic, J.; Berman, D.S.; et al. Atherosclerotic Plaque Characterization by CT Angiography for Identification of High-Risk Coronary Artery Lesions: A Comparison to Optical Coherence Tomography. *Eur. Heart J.—Cardiovasc. Imaging* **2015**, *16*, 373–379. [CrossRef] [PubMed]
27. Hoffmann, U.; Moselewski, F.; Nieman, K.; Jang, I.-K.; Ferencik, M.; Rahman, A.M.; Cury, R.C.; Abbara, S.; Joneidi-Jafari, H.; Achenbach, S.; et al. Noninvasive Assessment of Plaque Morphology and Composition in Culprit and Stable Lesions in Acute Coronary Syndrome and Stable Lesions in Stable Angina by Multidetector Computed Tomography. *J. Am. Coll. Cardiol.* **2006**, *47*, 1655–1662. [CrossRef]
28. Ahmadi, A.; Leipsic, J.; Øvrehus, K.A.; Gaur, S.; Bagiella, E.; Ko, B.; Dey, D.; LaRocca, G.; Jensen, J.M.; Bøtker, H.E.; et al. Lesion-Specific and Vessel-Related Determinants of Fractional Flow Reserve beyond Coronary Artery Stenosis. *JACC Cardiovasc. Imaging* **2018**, *11*, 521–530. [CrossRef]
29. Motoyama, S.; Ito, H.; Sarai, M.; Kondo, T.; Kawai, H.; Nagahara, Y.; Harigaya, H.; Kan, S.; Anno, H.; Takahashi, H.; et al. Plaque Characterization by Coronary Computed Tomography Angiography and the Likelihood of Acute Coronary Events in Mid-Term Follow-Up. *J. Am. Coll. Cardiol.* **2015**, *66*, 337–346. [CrossRef]
30. Williams, M.C.; Moss, A.J.; Dweck, M.; Adamson, P.D.; Alam, S.; Hunter, A.; Shah, A.S.V.; Pawade, T.; Weir-McCall, J.R.; Roditi, G.; et al. Coronary Artery Plaque Characteristics Associated with Adverse Outcomes in the SCOT-HEART Study. *J. Am. Coll. Cardiol.* **2019**, *73*, 291–301. [CrossRef]

31. Cury, R.C.; Abbara, S.; Achenbach, S.; Agatston, A.; Berman, D.S.; Budoff, M.J.; Dill, K.E.; Jacobs, J.E.; Maroules, C.D.; Rubin, G.D.; et al. CAD-RADSTM Coronary Artery Disease—Reporting and Data System. An Expert Consensus Document of the Society of Cardiovascular Computed Tomography (SCCT), the American College of Radiology (ACR) and the North American Society for Cardiovascular Imaging (NASCI). *J. Cardiovasc. Comput. Tomogr.* **2016**, *10*, 269–281. [CrossRef]
32. Kalisz, K.; Buethe, J.; Saboo, S.S.; Abbara, S.; Halliburton, S.; Rajiah, P. Artifacts at Cardiac CT: Physics and Solutions. *RadioGraphics* **2016**, *36*, 2064–2083. [CrossRef] [PubMed]
33. Liu, H.; Wingert, A.; Wang, J.; Zhang, J.; Wang, X.; Sun, J.; Chen, F.; Khalid, S.G.; Jiang, J.; Zheng, D. Extraction of Coronary Atherosclerotic Plaques from Computed Tomography Imaging: A Review of Recent Methods. *Front. Cardiovasc. Med.* **2021**, *8*, 597568. [CrossRef] [PubMed]
34. Liu, H.; Wingert, A.; Wang, X.; Zhang, J.; Sun, J.; Chen, F.; Khalid, S.G.; Gong, Y.; Xia, L.; Jiang, J.; et al. Consistency in Geometry among Coronary Atherosclerotic Plaques Extracted from Computed Tomography Angiography. *Front. Physiol.* **2021**, *12*, 715265. [CrossRef] [PubMed]
35. Dai, T.; Wang, J.; Hu, P. Diagnostic Performance of Computed Tomography Angiography in the Detection of Coronary Artery In-Stent Restenosis: Evidence from an Updated Meta-Analysis. *Eur. Radiol.* **2018**, *28*, 1373–1382. [CrossRef] [PubMed]
36. Chan, M.; Ridley, L.; Dunn, D.J.; Tian, D.H.; Liou, K.; Ozdirik, J.; Cheruvu, C.; Cao, C. A Systematic Review and Meta-Analysis of Multidetector Computed Tomography in the Assessment of Coronary Artery Bypass Grafts. *Int. J. Cardiol.* **2016**, *221*, 898–905. [CrossRef]
37. De Graaf, F.R.; van Velzen, J.E.; Witkowska, A.J.; Schuijf, J.D.; van der Bijl, N.; Kroft, L.J.; de Roos, A.; Reiber, J.H.C.; Bax, J.J.; de Grooth, G.J.; et al. Diagnostic Performance of 320-Slice Multidetector Computed Tomography Coronary Angiography in Patients after Coronary Artery Bypass Grafting. *Eur. Radiol.* **2011**, *21*, 2285–2296. [CrossRef]
38. Gupta, A.; Bera, K.; Kikano, E.; Pierce, J.D.; Gan, J.; Rajdev, M.; Ciancibello, L.M.; Gupta, A.; Rajagopalan, S.; Gilkeson, R.C. Coronary Artery Calcium Scoring: Current Status and Future Directions. *RadioGraphics* **2022**, *42*, 947–967. [CrossRef]
39. Greenland, P.; Bonow, R.O.; Brundage, B.H.; Budoff, M.J.; Eisenberg, M.J.; Grundy, S.M.; Lauer, M.S.; Post, W.S.; Raggi, P.; Redberg, R.F.; et al. ACCF/AHA 2007 Clinical Expert Consensus Document on Coronary Artery Calcium Scoring by Computed Tomography in Global Cardiovascular Risk Assessment and in Evaluation of Patients with Chest Pain. *Circulation* **2007**, *115*, 402–426. [CrossRef]
40. Shah, N.R.; Coulter, S.A. An Evidence-Based Guide for Coronary Calcium Scoring in Asymptomatic Patients without Coronary Heart Disease. *Tex. Heart Inst. J.* **2012**, *39*, 240–242.
41. McCollough, C.H.; Ulzheimer, S.; Halliburton, S.S.; Shanneik, K.; White, R.D.; Kalender, W.A. Coronary Artery Calcium: A Multi-Institutional, Multimanufacturer International Standard for Quantification at Cardiac CT. *Radiology* **2007**, *243*, 527–538. [CrossRef]
42. Sandfort, V.; Bluemke, D.A. CT Calcium Scoring. History, Current Status and Outlook. *Diagn. Interv. Imaging* **2017**, *98*, 3–10. [CrossRef] [PubMed]
43. Agatston, A.S.; Janowitz, W.R.; Hildner, F.J.; Zusmer, N.R.; Viamonte, M.; Detrano, R. Quantification of Coronary Artery Calcium Using Ultrafast Computed Tomography. *J. Am. Coll. Cardiol.* **1990**, *15*, 827–832. [CrossRef] [PubMed]
44. Budoff, M.J.; Nasir, K.; McClelland, R.L.; Detrano, R.; Wong, N.; Blumenthal, R.S.; Kondos, G.; Kronmal, R.A. Coronary Calcium Predicts Events Better with Absolute Calcium Scores Than Age-Sex-Race/Ethnicity Percentiles. *J. Am. Coll. Cardiol.* **2009**, *53*, 345–352. [CrossRef] [PubMed]
45. Perrone-Filardi, P.; Achenbach, S.; Mohlenkamp, S.; Reiner, Z.; Sambuceti, G.; Schuijf, J.D.; Van der Wall, E.; Kaufmann, P.A.; Knuuti, J.; Schroeder, S.; et al. Cardiac Computed Tomography and Myocardial Perfusion Scintigraphy for Risk Stratification in Asymptomatic Individuals without Known Cardiovascular Disease: A Position Statement of the Working Group on Nuclear Cardiology and Cardiac CT of the European Soci. *Eur. Heart J.* **2011**, *32*, 1986–1993. [CrossRef] [PubMed]
46. Callister, T.Q.; Cooil, B.; Raya, S.P.; Lippolis, N.J.; Russo, D.J.; Raggi, P. Coronary Artery Disease: Improved Reproducibility of Calcium Scoring with an Electron-Beam CT Volumetric Method. *Radiology* **1998**, *208*, 807–814. [CrossRef]
47. Brown, E.R.; Kronmal, R.A.; Bluemke, D.A.; Guerci, A.D.; Carr, J.J.; Goldin, J.; Detrano, R. Coronary Calcium Coverage Score: Determination, Correlates, and Predictive Accuracy in the Multi-Ethnic Study of Atherosclerosis. *Radiology* **2008**, *247*, 669–675. [CrossRef]
48. Shekar, C.; Budoff, M. Calcification of the Heart: Mechanisms and Therapeutic Avenues. *Expert Rev. Cardiovasc. Ther.* **2018**, *16*, 527–536. [CrossRef]
49. Proudfoot, D.; Shanahan, C.M. Biology of Calcification in Vascular Cells: Intima versus Media. *Herz* **2001**, *26*, 245–251. [CrossRef]
50. Tintut, Y.; Alfonso, Z.; Saini, T.; Radcliff, K.; Watson, K.; Boström, K.; Demer, L.L. Multilineage Potential of Cells from the Artery Wall. *Circulation* **2003**, *108*, 2505–2510. [CrossRef]
51. Tyson, K.L.; Reynolds, J.L.; McNair, R.; Zhang, Q.; Weissberg, P.L.; Shanahan, C.M. Osteo/Chondrocytic Transcription Factors and Their Target Genes Exhibit Distinct Patterns of Expression in Human Arterial Calcification. *Arterioscler. Thromb. Vasc. Biol.* **2003**, *23*, 489–494. [CrossRef]
52. Nusca, A.; Viscusi, M.M.; Piccirillo, F.; De Filippis, A.; Nenna, A.; Spadaccio, C.; Nappi, F.; Chello, C.; Mangiacapra, F.; Grigioni, F.; et al. In Stent Neo-Atherosclerosis: Pathophysiology, Clinical Implications, Prevention, and Therapeutic Approaches. *Life* **2022**, *12*, 393. [CrossRef] [PubMed]

53. Bear, M.; Butcher, M.; Shaughnessy, S.G. Oxidized Low-Density Lipoprotein Acts Synergistically with β-Glycerophosphate to Induce Osteoblast Differentiation in Primary Cultures of Vascular Smooth Muscle Cells. *J. Cell. Biochem.* **2008**, *105*, 185–193. [CrossRef] [PubMed]
54. Piccirillo, F.; Carpenito, M.; Verolino, G.; Chello, C.; Nusca, A.; Lusini, M.; Spadaccio, C.; Nappi, F.; Di Sciascio, G.; Nenna, A. Changes of the Coronary Arteries and Cardiac Microvasculature with Aging: Implications for Translational Research and Clinical Practice. *Mech. Ageing Dev.* **2019**, *184*, 111161. [CrossRef] [PubMed]
55. Maher, J.E.; Raz, J.A.; Bielak, L.F.; Sheecly, P.F.; Schwartz, R.S.; Peyser, P.A. Potential of Quantity of Coronary Artery Calcification to Identify New Risk Factors for Asymptomatic Atherosclerosis. *Am. J. Epidemiol.* **1996**, *144*, 943–953. [CrossRef] [PubMed]
56. Taylor, A.J.; Feuerstein, I.; Wong, H.; Barko, W.; Brazaitis, M.; O'Malley, P.G. Do Conventional Risk Factors Predict Subclinical Coronary Artery Disease? Results from the Prospective Army Coronary Calcium Project. *Am. Heart J.* **2001**, *141*, 463–468. [CrossRef] [PubMed]
57. Chen, N.X.; Duan, D.; O'Neill, K.D.; Moe, S.M. High Glucose Increases the Expression of Cbfa1 and BMP-2 and Enhances the Calcification of Vascular Smooth Muscle Cells. *Nephrol. Dial. Transplant.* **2006**, *21*, 3435–3442. [CrossRef]
58. Burke, A.P.; Farb, A.; Malcom, G.T.; Liang, Y.; Smialek, J.; Virmani, R. Effect of Risk Factors on the Mechanism of Acute Thrombosis and Sudden Coronary Death in Women. *Circulation* **1998**, *97*, 2110–2116. [CrossRef]
59. Erbel, R.; Möhlenkamp, S.; Moebus, S.; Schmermund, A.; Lehmann, N.; Stang, A.; Dragano, N.; Grönemeyer, D.; Seibel, R.; Kälsch, H.; et al. Coronary Risk Stratification, Discrimination, and Reclassification Improvement Based on Quantification of Subclinical Coronary Atherosclerosis. *J. Am. Coll. Cardiol.* **2010**, *56*, 1397–1406. [CrossRef]
60. Vliegenthart, R.; Oudkerk, M.; Hofman, A.; Oei, H.-H.S.; van Dijck, W.; van Rooij, F.J.A.; Witteman, J.C.M. Coronary Calcification Improves Cardiovascular Risk Prediction in the Elderly. *Circulation* **2005**, *112*, 572–577. [CrossRef]
61. Sarwar, A.; Shaw, L.J.; Shapiro, M.D.; Blankstein, R.; Hoffman, U.; Cury, R.C.; Abbara, S.; Brady, T.J.; Budoff, M.J.; Blumenthal, R.S.; et al. Diagnostic and Prognostic Value of Absence of Coronary Artery Calcification. *JACC Cardiovasc. Imaging* **2009**, *2*, 675–688. [CrossRef]
62. Peng, A.W.; Mirbolouk, M.; Orimoloye, O.A.; Osei, A.D.; Dardari, Z.; Dzaye, O.; Budoff, M.J.; Shaw, L.; Miedema, M.D.; Rumberger, J.; et al. Long-Term All-Cause and Cause-Specific Mortality in Asymptomatic Patients with CAC ≥ 1000. *JACC Cardiovasc. Imaging* **2020**, *13*, 83–93. [CrossRef] [PubMed]
63. Greenland, P. Coronary Artery Calcium Score Combined with Framingham Score for Risk Prediction in Asymptomatic Individuals. *JAMA* **2004**, *291*, 210. [CrossRef] [PubMed]
64. Arad, Y.; Goodman, K.J.; Roth, M.; Newstein, D.; Guerci, A.D. Coronary Calcification, Coronary Disease Risk Factors, C-Reactive Protein, and Atherosclerotic Cardiovascular Disease Events. *J. Am. Coll. Cardiol.* **2005**, *46*, 158–165. [CrossRef] [PubMed]
65. Greenland, P.; Blaha, M.J.; Budoff, M.J.; Erbel, R.; Watson, K.E. Coronary Calcium Score and Cardiovascular Risk. *J. Am. Coll. Cardiol.* **2018**, *72*, 434–447. [CrossRef]
66. Ajufo, E.; Ayers, C.R.; Vigen, R.; Joshi, P.H.; Rohatgi, A.; de Lemos, J.A.; Khera, A. Value of Coronary Artery Calcium Scanning in Association with the Net Benefit of Aspirin in Primary Prevention of Atherosclerotic Cardiovascular Disease. *JAMA Cardiol.* **2021**, *6*, 179. [CrossRef]
67. Budoff, M.J.; Dowe, D.; Jollis, J.G.; Gitter, M.; Sutherland, J.; Halamert, E.; Scherer, M.; Bellinger, R.; Martin, A.; Benton, R.; et al. Diagnostic Performance of 64-Multidetector Row Coronary Computed Tomographic Angiography for Evaluation of Coronary Artery Stenosis in Individuals without Known Coronary Artery Disease. *J. Am. Coll. Cardiol.* **2008**, *52*, 1724–1732. [CrossRef]
68. Meijboom, W.B.; van Mieghem, C.A.G.; Mollet, N.R.; Pugliese, F.; Weustink, A.C.; van Pelt, N.; Cademartiri, F.; Nieman, K.; Boersma, E.; de Jaegere, P.; et al. 64-Slice Computed Tomography Coronary Angiography in Patients with High, Intermediate, or Low Pretest Probability of Significant Coronary Artery Disease. *J. Am. Coll. Cardiol.* **2007**, *50*, 1469–1475. [CrossRef]
69. Winther, S.; Schmidt, S.E.; Mayrhofer, T.; Bøtker, H.E.; Hoffmann, U.; Douglas, P.S.; Wijns, W.; Bax, J.; Nissen, L.; Lynggaard, V.; et al. Incorporating Coronary Calcification into Pre-Test Assessment of the Likelihood of Coronary Artery Disease. *J. Am. Coll. Cardiol.* **2020**, *76*, 2421–2432. [CrossRef]
70. Sow, M.A.; Magne, J.; Salle, L.; Nobecourt, E.; Preux, P.-M.; Aboyans, V. Prevalence, Determinants and Prognostic Value of High Coronary Artery Calcium Score in Asymptomatic Patients with Diabetes: A Systematic Review and Meta-Analysis. *J. Diabetes Complicat.* **2022**, *36*, 108237. [CrossRef]
71. Wang, F.M.; Rozanski, A.; Arnson, Y.; Budoff, M.J.; Miedema, M.D.; Nasir, K.; Shaw, L.J.; Rumberger, J.A.; Blumenthal, R.S.; Matsushita, K.; et al. Cardiovascular and All-Cause Mortality Risk by Coronary Artery Calcium Scores and Percentiles among Older Adult Males and Females. *Am. J. Med.* **2021**, *134*, 341–350. [CrossRef]
72. Block, G.A.; Raggi, P.; Bellasi, A.; Kooienga, L.; Spiegel, D.M. Mortality Effect of Coronary Calcification and Phosphate Binder Choice in Incident Hemodialysis Patients. *Kidney Int.* **2007**, *71*, 438–441. [CrossRef] [PubMed]
73. Gassett, A.J.; Sheppard, L.; McClelland, R.L.; Olives, C.; Kronmal, R.; Blaha, M.J.; Budoff, M.; Kaufman, J.D. Risk Factors for Long-Term Coronary Artery Calcium Progression in the Multi-Ethnic Study of Atherosclerosis. *J. Am. Heart Assoc.* **2015**, *4*, e001726. [CrossRef] [PubMed]
74. Schindler, T.H.; Cadenas, J.; Facta, A.D.; Li, Y.; Olschewski, M.; Sayre, J.; Goldin, J.; Schelbert, H.R. Improvement in Coronary Endothelial Function Is Independently Associated with a Slowed Progression of Coronary Artery Calcification in Type 2 Diabetes Mellitus. *Eur. Heart J.* **2009**, *30*, 3064–3073. [CrossRef] [PubMed]

75. Raggi, P.; Callister, T.Q.; Shaw, L.J. Progression of Coronary Artery Calcium and Risk of First Myocardial Infarction in Patients Receiving Cholesterol-Lowering Therapy. *Arterioscler. Thromb. Vasc. Biol.* **2004**, *24*, 1272–1277. [CrossRef]
76. Budoff, M.J.; Young, R.; Lopez, V.A.; Kronmal, R.A.; Nasir, K.; Blumenthal, R.S.; Detrano, R.C.; Bild, D.E.; Guerci, A.D.; Liu, K.; et al. Progression of Coronary Calcium and Incident Coronary Heart Disease Events. *J. Am. Coll. Cardiol.* **2013**, *61*, 1231–1239. [CrossRef]
77. Radford, N.B.; DeFina, L.F.; Barlow, C.E.; Lakoski, S.G.; Leonard, D.; Paixao, A.R.M.; Khera, A.; Levine, B.D. Progression of CAC Score and Risk of Incident CVD. *JACC Cardiovasc. Imaging* **2016**, *9*, 1420–1429. [CrossRef]
78. Lehmann, N.; Erbel, R.; Mahabadi, A.A.; Rauwolf, M.; Möhlenkamp, S.; Moebus, S.; Kälsch, H.; Budde, T.; Schmermund, A.; Stang, A.; et al. Value of Progression of Coronary Artery Calcification for Risk Prediction of Coronary and Cardiovascular Events. *Circulation* **2018**, *137*, 665–679. [CrossRef]
79. Hecht, H.S.; Cronin, P.; Blaha, M.J.; Budoff, M.J.; Kazerooni, E.A.; Narula, J.; Yankelevitz, D.; Abbara, S. 2016 SCCT/STR Guidelines for Coronary Artery Calcium Scoring of Noncontrast Noncardiac Chest CT Scans: A Report of the Society of Cardiovascular Computed Tomography and Society of Thoracic Radiology. *J. Cardiovasc. Comput. Tomogr.* **2017**, *11*, 74–84. [CrossRef]
80. Zang, Y.; Dai, L.; Zhang, Y.; Xia, L. One-Dimensional Simulation of Transmural Heterogeneity of Cardiac Cellular Electromechanics. *Comput. Cardiol.* **2011**, *38*, 65–68.
81. Huang, A.L.; Maggiore, P.L.; Brown, R.A.; Turaga, M.; Reid, A.B.; Merkur, J.; Blanke, P.; Leipsic, J.A. CT-Derived Fractional Flow Reserve (FFR CT): From Gatekeeping to Roadmapping. *Can. Assoc. Radiol. J.* **2020**, *71*, 201–207. [CrossRef]
82. Zhao, X.; Zhang, J.; Gong, Y.; Xu, L.; Liu, H.; Wei, S.; Wu, Y.; Cha, G.; Wei, H.; Mao, J.; et al. Reliable Detection of Myocardial Ischemia Using Machine Learning Based on Temporal-Spatial Characteristics of Electrocardiogram and Vectorcardiogram. *Front. Physiol.* **2022**, *13*, 854191. [CrossRef] [PubMed]
83. He, J.; Tse, G.; Korantzopoulos, P.; Letsas, K.P.; Ali-Hasan-Al-Saegh, S.; Kamel, H.; Li, G.; Lip, G.Y.H.; Liu, T. P-Wave Indices and Risk of Ischemic Stroke. *Stroke* **2017**, *48*, 2066–2072. [CrossRef] [PubMed]
84. Tse, G.; Wong, C.W.; Gong, M.Q.; Meng, L.; Letsas, K.P.; Li, G.P.; Whittaker, P.; Bhardwaj, A.; Sawant, A.C.; Wu, W.K.; et al. Meta-Analysis of T-Wave Indices for Risk Stratification in Myocardial Infarction. *J. Geriatr. Cardiol.* **2017**, *14*, 776–779. [PubMed]
85. Dou, J.; Xia, L.; Deng, D.; Zang, Y.; Shou, G.; Bustos, C.; Tu, W.; Liu, F.; Crozier, S. A Study of Mechanical Optimization Strategy for Cardiac Resynchronization Therapy Based on an Electromechanical Model. *Comput. Math. Methods Med.* **2012**, *2012*, 948781. [CrossRef]
86. Geng, Y.; Wu, X.; Liu, H.; Zheng, D.; Xia, L. Index of Microcirculatory Resistance: State-of-the-Art and Potential Applications in Computational Simulation of Coronary Artery Disease. *J. Zhejiang Univ. B* **2022**, *23*, 123–140. [CrossRef]
87. Geng, Y.; Liu, H.; Wang, X.; Zhang, J.; Gong, Y.; Zheng, D.; Jiang, J.; Xia, L. Effect of Microcirculatory Dysfunction on Coronary Hemodynamics: A Pilot Study Based on Computational Fluid Dynamics Simulation. *Comput. Biol. Med.* **2022**, *146*, 105583. [CrossRef]
88. Yeung, C.; Baranchuk, A.; Tse, G.; Liu, T. The Importance of Measuring Coronary Blood Flow for Clinical Decision Making. *Curr. Cardiol. Rev.* **2019**, *15*, 320–321. [CrossRef]
89. Rizvi, A.; Han, D.; Danad, I.; Ó Hartaigh, B.; Lee, J.H.; Gransar, H.; Stuijfzand, W.J.; Roudsari, H.M.; Park, M.W.; Szymonifka, J.; et al. Diagnostic Performance of Hybrid Cardiac Imaging Methods for Assessment of Obstructive Coronary Artery Disease Compared with Stand-Alone Coronary Computed Tomography Angiography. *JACC Cardiovasc. Imaging* **2018**, *11*, 589–599. [CrossRef]
90. Hyafil, F.; Jaber, W.A.; Neglia, D. Highlights of the 14th International Conference on Nuclear Cardiology and Cardiac Computed Tomography. *Eur. Heart J.—Cardiovasc. Imaging* **2019**, *21*, 1–9. [CrossRef]
91. Le Jemtel, T.H.; Samson, R.; Ayinapudi, K.; Singh, T.; Oparil, S. Epicardial Adipose Tissue and Cardiovascular Disease. *Curr. Hypertens. Rep.* **2019**, *21*, 36. [CrossRef]
92. Sacks, H.S.; Fain, J.N. Human Epicardial Adipose Tissue: A Review. *Am. Heart J.* **2007**, *153*, 907–917. [CrossRef] [PubMed]
93. Iacobellis, G.; Corradi, D.; Sharma, A.M. Epicardial Adipose Tissue: Anatomic, Biomolecular and Clinical Relationships with the Heart. *Nat. Clin. Pract. Cardiovasc. Med.* **2005**, *2*, 536–543. [CrossRef] [PubMed]
94. Antonopoulos, A.S.; Sanna, F.; Sabharwal, N.; Thomas, S.; Oikonomou, E.K.; Herdman, L.; Margaritis, M.; Shirodaria, C.; Kampoli, A.-M.; Akoumianakis, I.; et al. Detecting Human Coronary Inflammation by Imaging Perivascular Fat. *Sci. Transl. Med.* **2017**, *9*, eaal2658. [CrossRef] [PubMed]
95. Mazurek, T.; Zhang, L.; Zalewski, A.; Mannion, J.D.; Diehl, J.T.; Arafat, H.; Sarov-Blat, L.; O'Brien, S.; Keiper, E.A.; Johnson, A.G.; et al. Human Epicardial Adipose Tissue Is a Source of Inflammatory Mediators. *Circulation* **2003**, *108*, 2460–2466. [CrossRef]
96. Rabkin, S.W. Epicardial Fat: Properties, Function and Relationship to Obesity. *Obes. Rev.* **2007**, *8*, 253–261. [CrossRef]
97. Lin, A.; Dey, D.; Wong, D.T.L.; Nerlekar, N. Perivascular Adipose Tissue and Coronary Atherosclerosis: From Biology to Imaging Phenotyping. *Curr. Atheroscler. Rep.* **2019**, *21*, 47. [CrossRef]
98. Chechi, K.; Richard, D. Thermogenic Potential and Physiological Relevance of Human Epicardial Adipose Tissue. *Int. J. Obes. Suppl.* **2015**, *5*, S28–S34. [CrossRef]
99. Hirata, Y.; Tabata, M.; Kurobe, H.; Motoki, T.; Akaike, M.; Nishio, C.; Higashida, M.; Mikasa, H.; Nakaya, Y.; Takanashi, S.; et al. Coronary Atherosclerosis Is Associated with Macrophage Polarization in Epicardial Adipose Tissue. *J. Am. Coll. Cardiol.* **2011**, *58*, 248–255. [CrossRef]

100. Demir, B.; Demir, E.; Acıksarı, G.; Uygun, T.; Utku, I.K.; Gedikbasi, A.; Caglar, I.M.; Pirhan, O.; Tureli, H.O.; Oflar, E.; et al. The Association between the Epicardial Adipose Tissue Thickness and Oxidative Stress Parameters in Isolated Metabolic Syndrome Patients: A Multimarker Approach. *Int. J. Endocrinol.* **2014**, *2014*, 954045. [CrossRef]
101. Baker, A.R.; Harte, A.L.; Howell, N.; Pritlove, D.C.; Ranasinghe, A.M.; da Silva, N.F.; Youssef, E.M.; Khunti, K.; Davies, M.J.; Bonser, R.S.; et al. Epicardial Adipose Tissue as a Source of Nuclear Factor-KB and c-Jun N-Terminal Kinase Mediated Inflammation in Patients with Coronary Artery Disease. *J. Clin. Endocrinol. Metab.* **2009**, *94*, 261–267. [CrossRef]
102. Nusca, A.; Piccirillo, F.; Bernardini, F.; De Filippis, A.; Coletti, F.; Mangiacapra, F.; Ricottini, E.; Melfi, R.; Gallo, P.; Cammalleri, V.; et al. Glycaemic Control in Patients Undergoing Percutaneous Coronary Intervention: What Is the Role for the Novel Antidiabetic Agents? A Comprehensive Review of Basic Science and Clinical Data. *Int. J. Mol. Sci.* **2022**, *23*, 7261. [CrossRef] [PubMed]
103. Montazerifar, F.; Bolouri, A.; Paghalea, R.S.; Mahani, M.K.; Karajibani, M. Obesity, Serum Resistin and Leptin Levels Linked to Coronary Artery Disease. *Arq. Bras. Cardiol.* **2016**, *107*, 348–353. [CrossRef] [PubMed]
104. Yafei, S.; Elsewy, F.; Youssef, E.; Ayman, M.; Elshafei, M.; Abayazeed, R. Echocardiographic Association of Epicardial Fat with Carotid Intima–Media Thickness in Patients with Type 2 Diabetes. *Diabetes Vasc. Dis. Res.* **2019**, *16*, 378–384. [CrossRef] [PubMed]
105. Militello, C.; Rundo, L.; Toia, P.; Conti, V.; Russo, G.; Filorizzo, C.; Maffei, E.; Cademartiri, F.; La Grutta, L.; Midiri, M.; et al. A Semi-Automatic Approach for Epicardial Adipose Tissue Segmentation and Quantification on Cardiac CT Scans. *Comput. Biol. Med.* **2019**, *114*, 103424. [CrossRef] [PubMed]
106. Mancio, J.; Azevedo, D.; Saraiva, F.; Azevedo, A.I.; Pires-Morais, G.; Leite-Moreira, A.; Falcao-Pires, I.; Lunet, N.; Bettencourt, N. Epicardial Adipose Tissue Volume Assessed by Computed Tomography and Coronary Artery Disease: A Systematic Review and Meta-Analysis. *Eur. Heart J.—Cardiovasc. Imaging* **2018**, *19*, 490–497. [CrossRef]
107. Wang, T.-D.; Lee, W.-J.; Shih, F.-Y.; Huang, C.-H.; Chang, Y.-C.; Chen, W.-J.; Lee, Y.-T.; Chen, M.-F. Relations of Epicardial Adipose Tissue Measured by Multidetector Computed Tomography to Components of the Metabolic Syndrome Are Region-Specific and Independent of Anthropometric Indexes and Intraabdominal Visceral Fat. *J. Clin. Endocrinol. Metab.* **2009**, *94*, 662–669. [CrossRef] [PubMed]
108. La Grutta, L.; Toia, P.; Farruggia, A.; Albano, D.; Grassedonio, E.; Palmeri, A.; Maffei, E.; Galia, M.; Vitabile, S.; Cademartiri, F.; et al. Quantification of Epicardial Adipose Tissue in Coronary Calcium Score and CT Coronary Angiography Image Data Sets: Comparison of Attenuation Values, Thickness and Volumes. *Br. J. Radiol.* **2016**, *89*, 20150773. [CrossRef]
109. Spearman, J.V.; Renker, M.; Schoepf, U.J.; Krazinski, A.W.; Herbert, T.L.; De Cecco, C.N.; Nietert, P.J.; Meinel, F.G. Prognostic Value of Epicardial Fat Volume Measurements by Computed Tomography: A Systematic Review of the Literature. *Eur. Radiol.* **2015**, *25*, 3372–3381. [CrossRef]
110. Bastarrika, G.; Broncano, J.; Schoepf, U.J.; Schwarz, F.; Lee, Y.S.; Abro, J.A.; Costello, P.; Zwerner, P.L. Relationship between Coronary Artery Disease and Epicardial Adipose Tissue Quantification at Cardiac CT. *Acad. Radiol.* **2010**, *17*, 727–734. [CrossRef]
111. Yu, W.; Liu, B.; Zhang, F.; Wang, J.; Shao, X.; Yang, X.; Shi, Y.; Wang, B.; Xu, Y.; Wang, Y. Association of Epicardial Fat Volume with Increased Risk of Obstructive Coronary Artery Disease in Chinese Patients with Suspected Coronary Artery Disease. *J. Am. Heart Assoc.* **2021**, *10*, e018080. [CrossRef]
112. Gitsioudis, G.; Schmahl, C.; Missiou, A.; Voss, A.; Schüssler, A.; Abdel-Aty, H.; Buss, S.J.; Mueller, D.; Vembar, M.; Bryant, M.; et al. Epicardial Adipose Tissue Is Associated with Plaque Burden and Composition and Provides Incremental Value for the Prediction of Cardiac Outcome. A Clinical Cardiac Computed Tomography Angiography Study. *PLoS ONE* **2016**, *11*, e0155120. [CrossRef] [PubMed]
113. Alexopoulos, N.; McLean, D.S.; Janik, M.; Arepalli, C.D.; Stillman, A.E.; Raggi, P. Epicardial Adipose Tissue and Coronary Artery Plaque Characteristics. *Atherosclerosis* **2010**, *210*, 150–154. [CrossRef] [PubMed]
114. Ito, T.; Suzuki, Y.; Ehara, M.; Matsuo, H.; Teramoto, T.; Terashima, M.; Nasu, K.; Kinoshita, Y.; Tsuchikane, E.; Suzuki, T.; et al. Impact of Epicardial Fat Volume on Coronary Artery Disease in Symptomatic Patients with a Zero Calcium Score. *Int. J. Cardiol.* **2013**, *167*, 2852–2858. [CrossRef] [PubMed]
115. Nerlekar, N.; Brown, A.J.; Muthalaly, R.G.; Talman, A.; Hettige, T.; Cameron, J.D.; Wong, D.T.L. Association of Epicardial Adipose Tissue and High-Risk Plaque Characteristics: A Systematic Review and Meta-Analysis. *J. Am. Heart Assoc.* **2017**, *6*, e006379. [CrossRef]
116. Otsuka, K.; Ishikawa, H.; Yamaura, H.; Shirasawa, K.; Kasayuki, N. Epicardial Adipose Tissue Volume Is Associated with Low-Attenuation Plaque Volume in Subjects with or without Increased Visceral Fat: A 3-Vessel Coronary Artery Analysis with CT Angiography. *Eur. Heart J.* **2021**, *42*. [CrossRef]
117. Yamashita, K.; Yamamoto, M.H.; Igawa, W.; Ono, M.; Kido, T.; Ebara, S.; Okabe, T.; Saito, S.; Amemiya, K.; Isomura, N.; et al. Association of Epicardial Adipose Tissue Volume and Total Coronary Plaque Burden in Patients with Coronary Artery Disease. *Int. Heart J.* **2018**, *59*, 1219–1226. [CrossRef]
118. Iwasaki, K.; Matsumoto, T.; Aono, H.; Furukawa, H.; Samukawa, M. Relationship between Epicardial Fat Measured by 64-Multidetector Computed Tomography and Coronary Artery Disease. *Clin. Cardiol.* **2011**, *34*, 166–171. [CrossRef]
119. Cosson, E.; Nguyen, M.T.; Rezgani, I.; Berkane, N.; Pinto, S.; Bihan, H.; Tatulashvili, S.; Taher, M.; Sal, M.; Soussan, M.; et al. Epicardial Adipose Tissue Volume and Myocardial Ischemia in Asymptomatic People Living with Diabetes: A Cross-Sectional Study. *Cardiovasc. Diabetol.* **2021**, *20*, 224. [CrossRef]

120. Franssens, B.T.; Nathoe, H.M.; Visseren, F.L.J.; van der Graaf, Y.; Leiner, T.; Algra, A.; van der Graaf, Y.; Grobbee, D.E.; Rutten, G.E.H.M.; Visseren, F.L.J.; et al. Relation of Epicardial Adipose Tissue Radiodensity to Coronary Artery Calcium on Cardiac Computed Tomography in Patients at High Risk for Cardiovascular Disease. *Am. J. Cardiol.* **2017**, *119*, 1359–1365. [CrossRef]
121. Goeller, M.; Achenbach, S.; Marwan, M.; Doris, M.K.; Cadet, S.; Commandeur, F.; Chen, X.; Slomka, P.J.; Gransar, H.; Cao, J.J.; et al. Epicardial Adipose Tissue Density and Volume Are Related to Subclinical Atherosclerosis, Inflammation and Major Adverse Cardiac Events in Asymptomatic Subjects. *J. Cardiovasc. Comput. Tomogr.* **2018**, *12*, 67–73. [CrossRef]
122. Eisenberg, E.; McElhinney, P.A.; Commandeur, F.; Chen, X.; Cadet, S.; Goeller, M.; Razipour, A.; Gransar, H.; Cantu, S.; Miller, R.J.H.; et al. Deep Learning–Based Quantification of Epicardial Adipose Tissue Volume and Attenuation Predicts Major Adverse Cardiovascular Events in Asymptomatic Subjects. *Circ. Cardiovasc. Imaging* **2020**, *13*, e009829. [CrossRef] [PubMed]
123. Fuller, B.; Garland, J.; Anne, S.; Beh, R.; McNevin, D.; Tse, R. Increased Epicardial Fat Thickness in Sudden Death From Stable Coronary Artery Atherosclerosis. *Am. J. Forensic Med. Pathol.* **2017**, *38*, 162–166. [CrossRef] [PubMed]
124. Mahabadi, A.A.; Berg, M.H.; Lehmann, N.; Kälsch, H.; Bauer, M.; Kara, K.; Dragano, N.; Moebus, S.; Jöckel, K.-H.; Erbel, R.; et al. Association of Epicardial Fat with Cardiovascular Risk Factors and Incident Myocardial Infarction in the General Population. *J. Am. Coll. Cardiol.* **2013**, *61*, 1388–1395. [CrossRef] [PubMed]
125. Gorter, P.M.; de Vos, A.M.; van der Graaf, Y.; Stella, P.R.; Doevendans, P.A.; Meijs, M.F.L.; Prokop, M.; Visseren, F.L.J. Relation of Epicardial and Pericoronary Fat to Coronary Atherosclerosis and Coronary Artery Calcium in Patients Undergoing Coronary Angiography. *Am. J. Cardiol.* **2008**, *102*, 380–385. [CrossRef] [PubMed]
126. Balcer, B.; Dykun, I.; Schlosser, T.; Forsting, M.; Rassaf, T.; Mahabadi, A.A. Pericoronary Fat Volume but Not Attenuation Differentiates Culprit Lesions in Patients with Myocardial Infarction. *Atherosclerosis* **2018**, *276*, 182–188. [CrossRef] [PubMed]
127. Ma, R.; van Assen, M.; Ties, D.; Pelgrim, G.J.; van Dijk, R.; Sidorenkov, G.; van Ooijen, P.M.A.; van der Harst, P.; Vliegenthart, R. Focal Pericoronary Adipose Tissue Attenuation Is Related to Plaque Presence, Plaque Type, and Stenosis Severity in Coronary CTA. *Eur. Radiol.* **2021**, *31*, 7251–7261. [CrossRef]
128. Nogic, J.; Kim, J.; Layland, J.; Chan, J.; Cheng, K.; Wong, D.; Brown, A. TCT-241 Pericoronary Adipose Tissue Is a Predictor of In-Stent Restenosis and Stent Failure in Patients Undergoing Coronary Artery Stent Insertion. *J. Am. Coll. Cardiol.* **2021**, *78*, B98. [CrossRef]
129. Kang, J.; Kim, Y.-C.; Park, J.J.; Kim, S.; Kang, S.-H.; Cho, Y.J.; Yoon, Y.E.; Oh, I.-Y.; Yoon, C.-H.; Suh, J.-W.; et al. Increased Epicardial Adipose Tissue Thickness Is a Predictor of New-Onset Diabetes Mellitus in Patients with Coronary Artery Disease Treated with High-Intensity Statins. *Cardiovasc. Diabetol.* **2018**, *17*, 10. [CrossRef]
130. Raggi, P.; Gadiyaram, V.; Zhang, C.; Chen, Z.; Lopaschuk, G.; Stillman, A.E. Statins Reduce Epicardial Adipose Tissue Attenuation Independent of Lipid Lowering: A Potential Pleiotropic Effect. *J. Am. Heart Assoc.* **2019**, *8*, e013104. [CrossRef]
131. Ziyrek, M.; Kahraman, S.; Ozdemir, E.; Dogan, A. Metformin Monotherapy Significantly Decreases Epicardial Adipose Tissue Thickness in Newly Diagnosed Type 2 Diabetes Patients. *Rev. Port. Cardiol.* **2019**, *38*, 419–423. [CrossRef]
132. Iacobellis, G.; Villasante Fricke, A.C. Effects of Semaglutide Versus Dulaglutide on Epicardial Fat Thickness in Subjects with Type 2 Diabetes and Obesity. *J. Endocr. Soc.* **2020**, *4*, bvz042. [CrossRef] [PubMed]
133. Iacobellis, G.; Mohseni, M.; Bianco, S.D.; Banga, P.K. Liraglutide Causes Large and Rapid Epicardial Fat Reduction. *Obesity* **2017**, *25*, 311–316. [CrossRef] [PubMed]
134. Sato, T.; Aizawa, Y.; Yuasa, S.; Kishi, S.; Fuse, K.; Fujita, S.; Ikeda, Y.; Kitazawa, H.; Takahashi, M.; Sato, M.; et al. The Effect of Dapagliflozin Treatment on Epicardial Adipose Tissue Volume. *Cardiovasc. Diabetol.* **2018**, *17*, 6. [CrossRef] [PubMed]
135. Desai, M.Y.; Cremer, P.C.; Schoenhagen, P. Thoracic Aortic Calcification. *JACC Cardiovasc. Imaging* **2018**, *11*, 1012–1026. [CrossRef]
136. Budoff, M.J.; Nasir, K.; Katz, R.; Takasu, J.; Carr, J.J.; Wong, N.D.; Allison, M.; Lima, J.A.C.; Detrano, R.; Blumenthal, R.S.; et al. Thoracic Aortic Calcification and Coronary Heart Disease Events: The Multi-Ethnic Study of Atherosclerosis (MESA). *Atherosclerosis* **2011**, *215*, 196–202. [CrossRef]
137. Allison, M.A.; Hsi, S.; Wassel, C.L.; Morgan, C.; Ix, J.H.; Wright, C.M.; Criqui, M.H. Calcified Atherosclerosis in Different Vascular Beds and the Risk of Mortality. *Arterioscler. Thromb. Vasc. Biol.* **2012**, *32*, 140–146. [CrossRef]
138. Rivera, J.J.; Nasir, K.; Katz, R.; Takasu, J.; Allison, M.; Wong, N.D.; Barr, R.G.; Carr, J.J.; Blumenthal, R.S.; Budoff, M.J. Relationship of Thoracic Aortic Calcium to Coronary Calcium and Its Progression (from the Multi-Ethnic Study of Atherosclerosis [MESA]). *Am. J. Cardiol.* **2009**, *103*, 1562–1567. [CrossRef]
139. El-Saed, A.; Sekikawa, A.; Edmundowicz, D.; Evans, R.W.; Sutton-Tyrrell, K.; Kadowaki, T.; Choo, J.; Takamiya, T.; Kuller, L.H. Coronary Calcification Is More Predictive of Carotid Intimal Medial Thickness in Black Compared to White Middle Aged Men. *Atherosclerosis* **2008**, *196*, 913–918. [CrossRef]
140. Kodama, Y.; Ng, C.S.; Wu, T.T.; Ayers, G.D.; Curley, S.A.; Abdalla, E.K.; Vauthey, J.N.; Charnsangavej, C. Comparison of CT Methods for Determining the Fat Content of the Liver. *Am. J. Roentgenol.* **2007**, *188*, 1307–1312. [CrossRef]
141. Cademartiri, F.; Sverzellati, N.; Guaricci, A.I.; Maffei, E. Fat and Cardiovascular Risk: The Role of Cardiac CT. *Eur. Heart J.—Cardiovasc. Imaging* **2016**, *17*, 1368–1369. [CrossRef]
142. Bos, D.; Leening, M.J.G. Leveraging the Coronary Calcium Scan beyond the Coronary Calcium Score. *Eur. Radiol.* **2018**, *28*, 3082–3087. [CrossRef] [PubMed]

143. Yki-Järvinen, H. Non-Alcoholic Fatty Liver Disease as a Cause and a Consequence of Metabolic Syndrome. *Lancet Diabetes Endocrinol.* **2014**, *2*, 901–910. [CrossRef] [PubMed]
144. Stahl, E.P.; Dhindsa, D.S.; Lee, S.K.; Sandesara, P.B.; Chalasani, N.P.; Sperling, L.S. Nonalcoholic Fatty Liver Disease and the Heart. *J. Am. Coll. Cardiol.* **2019**, *73*, 948–963. [CrossRef] [PubMed]
145. Sung, K.-C.; Wild, S.H.; Kwag, H.J.; Byrne, C.D. Fatty Liver, Insulin Resistance, and Features of Metabolic Syndrome. *Diabetes Care* **2012**, *35*, 2359–2364. [CrossRef]
146. Puchner, S.B.; Lu, M.T.; Mayrhofer, T.; Liu, T.; Pursnani, A.; Ghoshhajra, B.B.; Truong, Q.A.; Wiviott, S.D.; Fleg, J.L.; Hoffmann, U.; et al. High-Risk Coronary Plaque at Coronary CT Angiography Is Associated with Nonalcoholic Fatty Liver Disease, Independent of Coronary Plaque and Stenosis Burden: Results from the ROMICAT II Trial. *Radiology* **2015**, *274*, 693–701. [CrossRef]
147. Wolff, L.; Bos, D.; Murad, S.D.; Franco, O.H.; Krestin, G.P.; Hofman, A.; Vernooij, M.W.; van der Lugt, A. Liver Fat Is Related to Cardiovascular Risk Factors and Subclinical Vascular Disease: The Rotterdam Study. *Eur. Heart J.—Cardiovasc. Imaging* **2016**, *17*, 1361–1367. [CrossRef]
148. Kotronen, A.; Yki-Järvinen, H. Fatty Liver. *Arterioscler. Thromb. Vasc. Biol.* **2008**, *28*, 27–38. [CrossRef]
149. Al Rifai, M.; Silverman, M.G.; Nasir, K.; Budoff, M.J.; Blankstein, R.; Szklo, M.; Katz, R.; Blumenthal, R.S.; Blaha, M.J. The Association of Nonalcoholic Fatty Liver Disease, Obesity, and Metabolic Syndrome, with Systemic Inflammation and Subclinical Atherosclerosis: The Multi-Ethnic Study of Atherosclerosis (MESA). *Atherosclerosis* **2015**, *239*, 629–633. [CrossRef]
150. Kannel, W.B.; Abbott, R.D. Incidence and Prognosis of Unrecognized Myocardial Infarction. *N. Engl. J. Med.* **1984**, *311*, 1144–1147. [CrossRef]
151. Madaj, P.; Budoff, M.J. Risk Stratification of Non-Contrast CT beyond the Coronary Calcium Scan. *J. Cardiovasc. Comput. Tomogr.* **2012**, *6*, 301–307. [CrossRef]
152. Kimura, F.; Matsuo, Y.; Nakajima, T.; Nishikawa, T.; Kawamura, S.; Sannohe, S.; Hagiwara, N.; Sakai, F. Myocardial Fat at Cardiac Imaging: How Can We Differentiate Pathologic from Physiologic Fatty Infiltration? *RadioGraphics* **2010**, *30*, 1587–1602. [CrossRef] [PubMed]
153. Zafar, H.M.; Litt, H.I.; Torigian, D.A. CT Imaging Features and Frequency of Left Ventricular Myocardial Fat in Patients with CT Findings of Chronic Left Ventricular Myocardial Infarction. *Clin. Radiol.* **2008**, *63*, 256–262. [CrossRef] [PubMed]
154. Ichikawa, Y.; Kitagawa, K.; Chino, S.; Ishida, M.; Matsuoka, K.; Tanigawa, T.; Nakamura, T.; Hirano, T.; Takeda, K.; Sakuma, H. Adipose Tissue Detected by Multislice Computed Tomography in Patients after Myocardial Infarction. *JACC Cardiovasc. Imaging* **2009**, *2*, 548–555. [CrossRef] [PubMed]
155. Nieman, K.; Cury, R.C.; Ferencik, M.; Nomura, C.H.; Abbara, S.; Hoffmann, U.; Gold, H.K.; Jang, I.-K.; Brady, T.J. Differentiation of Recent and Chronic Myocardial Infarction by Cardiac Computed Tomography. *Am. J. Cardiol.* **2006**, *98*, 303–308. [CrossRef]
156. Gupta, M.; Kadakia, J.; Hacioglu, Y.; Ahmadi, N.; Patel, A.; Choi, T.; Yamada, G.; Budoff, M. Non-Contrast Cardiac Computed Tomography Can Accurately Detect Chronic Myocardial Infarction: Validation Study. *J. Nucl. Cardiol.* **2011**, *18*, 96–103. [CrossRef]
157. Ko, S.M.; Hwang, S.H.; Lee, H.-J. Role of Cardiac Computed Tomography in the Diagnosis of Left Ventricular Myocardial Diseases. *J. Cardiovasc. Imaging* **2019**, *27*, 73. [CrossRef]
158. Lardo, A.C.; Cordeiro, M.A.S.; Silva, C.; Amado, L.C.; George, R.T.; Saliaris, A.P.; Schuleri, K.H.; Fernandes, V.R.; Zviman, M.; Nazarian, S.; et al. Contrast-Enhanced Multidetector Computed Tomography Viability Imaging after Myocardial Infarction. *Circulation* **2006**, *113*, 394–404. [CrossRef]
159. Mahnken, A.H.; Koos, R.; Katoh, M.; Wildberger, J.E.; Spuentrup, E.; Buecker, A.; Günther, R.W.; Kühl, H.P. Assessment of Myocardial Viability in Reperfused Acute Myocardial Infarction Using 16-Slice Computed Tomography in Comparison to Magnetic Resonance Imaging. *J. Am. Coll. Cardiol.* **2005**, *45*, 2042–2047. [CrossRef]
160. Gerber, B.L.; Belge, B.; Legros, G.J.; Lim, P.; Poncelet, A.; Pasquet, A.; Gisellu, G.; Coche, E.; Vanoverschelde, J.-L.J. Characterization of Acute and Chronic Myocardial Infarcts by Multidetector Computed Tomography. *Circulation* **2006**, *113*, 823–833. [CrossRef]
161. Palmisano, A.; Vignale, D.; Tadic, M.; Moroni, F.; De Stefano, D.; Gatti, M.; Boccia, E.; Faletti, R.; Oppizzi, M.; Peretto, G.; et al. Myocardial Late Contrast Enhancement CT in Troponin-Positive Acute Chest Pain Syndrome. *Radiology* **2022**, *302*, 545–553. [CrossRef]
162. Bouleti, C.; Baudry, G.; Iung, B.; Arangalage, D.; Abtan, J.; Ducrocq, G.; Steg, P.-G.; Vahanian, A.; Henry-Feugeas, M.-C.; Pasi, N.; et al. Usefulness of Late Iodine Enhancement on Spectral CT in Acute Myocarditis. *JACC Cardiovasc. Imaging* **2017**, *10*, 826–827. [CrossRef] [PubMed]
163. Esposito, A.; Palmisano, A.; Antunes, S.; Maccabelli, G.; Colantoni, C.; Rancoita, P.M.V.; Baratto, F.; Di Serio, C.; Rizzo, G.; De Cobelli, F.; et al. Cardiac CT with Delayed Enhancement in the Characterization of Ventricular Tachycardia Structural Substrate. *JACC Cardiovasc. Imaging* **2016**, *9*, 822–832. [CrossRef] [PubMed]
164. Treibel, T.A.; Fontana, M.; Steeden, J.A.; Nasis, A.; Yeung, J.; White, S.K.; Sivarajan, S.; Punwani, S.; Pugliese, F.; Taylor, S.A.; et al. Automatic Quantification of the Myocardial Extracellular Volume by Cardiac Computed Tomography: Synthetic ECV by CCT. *J. Cardiovasc. Comput. Tomogr.* **2017**, *11*, 221–226. [CrossRef] [PubMed]
165. Lee, H.-J.; Im, D.J.; Youn, J.-C.; Chang, S.; Suh, Y.J.; Hong, Y.J.; Kim, Y.J.; Hur, J.; Choi, B.W. Myocardial Extracellular Volume Fraction with Dual-Energy Equilibrium Contrast-Enhanced Cardiac CT in Nonischemic Cardiomyopathy: A Prospective Comparison with Cardiac MR Imaging. *Radiology* **2016**, *280*, 49–57. [CrossRef] [PubMed]

166. Treibel, T.A.; Bandula, S.; Fontana, M.; White, S.K.; Gilbertson, J.A.; Herrey, A.S.; Gillmore, J.D.; Punwani, S.; Hawkins, P.N.; Taylor, S.A.; et al. Extracellular Volume Quantification by Dynamic Equilibrium Cardiac Computed Tomography in Cardiac Amyloidosis. *J. Cardiovasc. Comput. Tomogr.* **2015**, *9*, 585–592. [CrossRef]
167. Richards, C.E.; Obaid, D.R. Low-Dose Radiation Advances in Coronary Computed Tomography Angiography in the Diagnosis of Coronary Artery Disease. *Curr. Cardiol. Rev.* **2019**, *15*, 304–315. [CrossRef]